

FEATURE ARTICLE

Biological Water: Femtosecond Dynamics of Macromolecular Hydration

Samir Kumar Pal, Jorge Peon, Biman Bagchi,[†] and Ahmed H. Zewail**Laboratory for Molecular Sciences, Arthur Amos Noyes Laboratory of Chemical Physics, California Institute of Technology, Pasadena, California 91125**Received: June 5, 2002; In Final Form: August 12, 2002*

The unique features of a macromolecule and water as a solvent make the issue of solvation unconventional, with questions about the static versus dynamic nature of hydration and the physics of orientational and translational diffusion at the boundary. For proteins, the hydration shell that covers the surface is critical to the stability of its structure and function. Dynamically speaking, the residence time of water at the surface is a signature of its mobility and binding. With femtosecond time resolution it is possible to unravel the shortest residence times which are key for the description of the hydration layer, static or dynamic. In this article we review these issues guided by experimental studies, from this laboratory, of polar hydration dynamics at the surfaces of two proteins (Subtilisin *Carlsberg* (SC) and Monellin). The natural probe tryptophan amino acid was used for the interrogation of the dynamics, and for direct comparison we also studied the behavior in bulk water—a complete hydration in 1 ps. We develop a theoretical description of solvation and relate the theory to the experimental observations. In this theoretical approach, we consider the dynamical equilibrium in the hydration shell, defining the rate processes for breaking and making the transient hydrogen bonds, and the effective friction in the layer which is defined by the translational and orientational motions of water molecules. The relationship between the residence time of water molecules and the observed slow component in solvation dynamics is a direct one. For the two proteins studied, we observed a “bimodal decay” for the hydration correlation function, with two primary relaxation times: ultrafast, typically 1 ps or less, and longer, typically 15–40 ps, and both are related to the residence time at the protein surface, depending on the binding energies. We end by making extensions to studies of the denatured state of the protein, random coils, and the biomimetic micelles, and conclude with our thoughts on the relevance of the dynamics of native structures to their functions.

I. Introduction

Biological macromolecules—proteins and DNA—are physiologically inactive without water. While many aspects of structure and dynamics of bulk water can be regarded as reasonably understood at present, the same is not true for the water which is found in interfacial or restricted environments, such as the surface of proteins or micelles. The water in the immediate vicinity of biomolecules (biological water) are particularly important to the structure and biological function. The focus of the present article is on the nature of this biological water and the associated dynamics at the molecular scale.¹

The water layer on such surfaces (or, inside the pool of a reverse micelle) is heterogeneous, even on a molecular length scale, and water properties in the layer are sensitive to the details of the interactions with the adjacent surface. In general, these interfacial structures and dynamics are fundamental to solvation,² molecular properties at interfaces,^{3,4} and the hydrophobic

bonding.⁵ For biological systems, different experimental and theoretical (mostly computer simulation) studies probe dynamics on different scales of length and time.⁶

For example, NMR studies give a range of residence times, sub-nanosecond 300–500 ps⁷ to 10–200 ps,⁸ while dielectric relaxation experiments have given time scales of the order of 10 ns⁹ (see below). NMR is sensitive to very short length scales of a few angstroms (with limited time resolution); dielectric relaxation averages all length scales. Solvation dynamics is sensitive to both time and length scales and can be a good probe of the dynamics of protein hydration (surface vs buried water) with femtosecond resolution, as discussed here for surface hydration and reported elsewhere for hydrophobic pockets/clefts (section III).

Recently, solvation dynamics studies have been reported¹⁰ using the natural probe tryptophan amino acid located at the protein surface. The results elucidated two types of solvation trajectories, bulk-type and protein-layer-type: both are dynamically reflective of the distribution in the residence times at the protein surface, as discussed in our report.¹⁰ The biological water indeed has a slower response time (38 ps for Subtilisin *Carlsberg* (SC) protein) than that of bulk hydration (~1ps) (for another

* To whom correspondence should be addressed. Email: zewail@caltech.edu. Fax: 626-796-8315.

[†] Permanent address: Solid State and Structural Chemistry Unit, Indian Institute of Science, Bangalore, 560012, India. Email: bbagchi@sscu.iisc.ernet.in.

protein, Monellin, the behavior is similar with a 16 ps relaxation time instead of 38 ps for SC, as discussed below). That is, the time scale is more than 1 order of magnitude longer than that of bulk water, but orders of magnitude smaller than that of dielectric measurements. To describe the range of time scales we must consider the molecular dynamics of water at the interface.

This article gives an overview of these recent experimental studies of solvation dynamics in two proteins (SC and Monellin) in the native and denatured state. We also discuss a simple theory, based on the assumption of a dynamic equilibrium^{2a} between the bound and the free states of water molecules in the hydration layer, which provides a relationship between the solvation correlation time and the residence time of water molecules. A correlation between the enhanced friction on a protein due to the slow water molecules in its hydration layer and the residence time is shown. We highlight the theoretical findings here, but more details will be published elsewhere.

One of the early indications that the hydration layer of a protein is different from the bulk water came from dielectric measurements.⁹ Three distinct regions in the frequency-dependent dielectric function were found, in contrast to one region for bulk water, suggesting different types of water dielectric properties. From these measurements it was found that the dielectric relaxation of a protein in solution (e.g., myoglobin ~ 10 ps, ~ 10 ns, and ~ 74 ns; see section V.B) contrasts that of bulk water (8.3 ps). The longer relaxation time, together with the Stokes expression of friction (from hydrodynamics), suggests a larger radius for the protein as a result of hydration. This gave rise to the conjecture of the existence of an “ice-like” static structure at the surface of the protein. This idea is now invalid. Information about biological water is derived from X-ray¹¹ and neutron diffraction,¹² and both indicate that in the crystalline form of a protein a significant number of water molecules are bound in the hydration sites. For example, the neutron diffraction study of ref 12 has shown that, for the protein carboxymyoglobin, 89 water molecules are well localized at specific hydration sites. As mentioned above, NMR studies have given a time scale for the dynamics, sub-nanosecond or shorter.

Several MD simulation studies have revealed the dynamical nature on the picosecond time scale. Stimulated by neutron diffraction experiments,¹² it was found recently¹³ by simulations that typically about 80% of the hydration sites of carboxymyoglobin are occupied by water molecules for a snapshot, and that only four water molecules remain bound during the entire length of the simulation (80 ps). The residence time of water molecules in the hydration layer of this protein was found to have a distribution between somewhat less than 30 ps to about 80 ps, which was the longest run time of the simulation.

The study found a strong peak in the radial distribution function for hydrogen bonding (energy from 0.5 to 9 kcal/mol) to the surface, suggesting a solvation shell at an average distance. The study of the trajectory of individual water molecules clearly shows two entirely different behaviors—one for the bound and the other for the free water. Rapid exchange between the two states of binding was evident in the MD suggesting the *existence of a dynamic equilibrium between the two states*. In another MD study of the dynamics of the protein plastocyanin,¹⁴ a survival correlation time for the hydration layers was defined. This correlation function was allowed to decay only when water molecules leave or enter the layer; the function was found to decay slowly for the molecules that are close to the surface of the protein. As importantly, it was also observed that the

rotational relaxation of the water molecules, on average, is significantly slowed in the close proximity of the protein surface.

One focus of this article is on the development of a simple description of the interface region which allows for the direct correlation to our experimental observables. In so doing, we relate residence times to solvation dynamics, define an effective friction caused by rotational and translational motions, and take into account the dynamical equilibrium between the bound and free water in the hydration layer. A potential energy of mean force as a function of the distance from the surface is given here to reproduce features of the distribution in residence times. These issues are discussed here guided by the reported experimental results on two proteins, native and denatured, and one biomimetic, a micelle.

In what follows, we first consider bulk hydration of the amino acid tryptophan, both theoretically and experimentally. Next, we consider protein hydration dynamics, also theoretically and experimentally. We end with the relevance of the findings for macromolecular hydration in the denatured state, and with some general conclusions.

II. Solvation Dynamics in Bulk Water

(A) Theoretical. To understand the meaning and scope of solvation dynamics, let us first visualize the physical essence of the dynamical process involved for a solute molecule in a polar solvent.¹⁵ A change in the solute is made at time $t = 0$, by femtosecond (fs) excitation, which leads to the creation of a dipole. This dipole gives rise to an instantaneous electric field on the solvent molecules. Because of the interaction of the solvent permanent dipoles with the electric field, the free energy minimum of the solvent shifts to a nonzero value of the polarization. The solvent motion is critical (Figure 1). Since the solute is excited instantaneously (a Franck–Condon transition as far the nuclear degrees of freedom are concerned), the solvent molecules at $t = 0$ find themselves in a relatively high-energy configuration. Subsequently, the solvent molecules begin to move and rearrange themselves to reach their new equilibrium positions (Figure 2). The nuclear motion involved can be broadly classified into rotational and translational motions.

When the solvent is bulk water, rotational motion would also include hindered rotation, libration, while translation would include the intermolecular vibration due to the extensive hydrogen bonding. The two specific motions, libration and intermolecular vibration, are relatively high in frequency and are expected to play a dominant role in the initial part of solvation.¹⁶ The molecular motions involved are shown schematically in Figure 1, and in Figure 3 we show a typical solvation time correlation function which we shall discuss below. For clarity, we approximate the motions responsible for decay in different regions.

A simple way to address the dynamics of polar solvation is to start with the following expression for the solvation energy $E_{\text{solv}}(t)$,^{15a}

$$E_{\text{solv}}(t) = -\frac{1}{2} \int d\mathbf{r} \mathbf{E}_0(\mathbf{r}) \cdot \mathbf{P}(\mathbf{r}, t) \quad (1)$$

where $\mathbf{E}_0(\mathbf{r})$ is the instantaneously created, position-dependent electric field from the ion or the dipole of the solute and $\mathbf{P}(\mathbf{r}, t)$ is the position- and time-dependent polarization. The latter is defined by the following expression:

$$\mathbf{P}(\mathbf{r}, t) = \int d\Omega \boldsymbol{\mu}(\Omega) \rho(\mathbf{r}, \Omega, t) \quad (2)$$

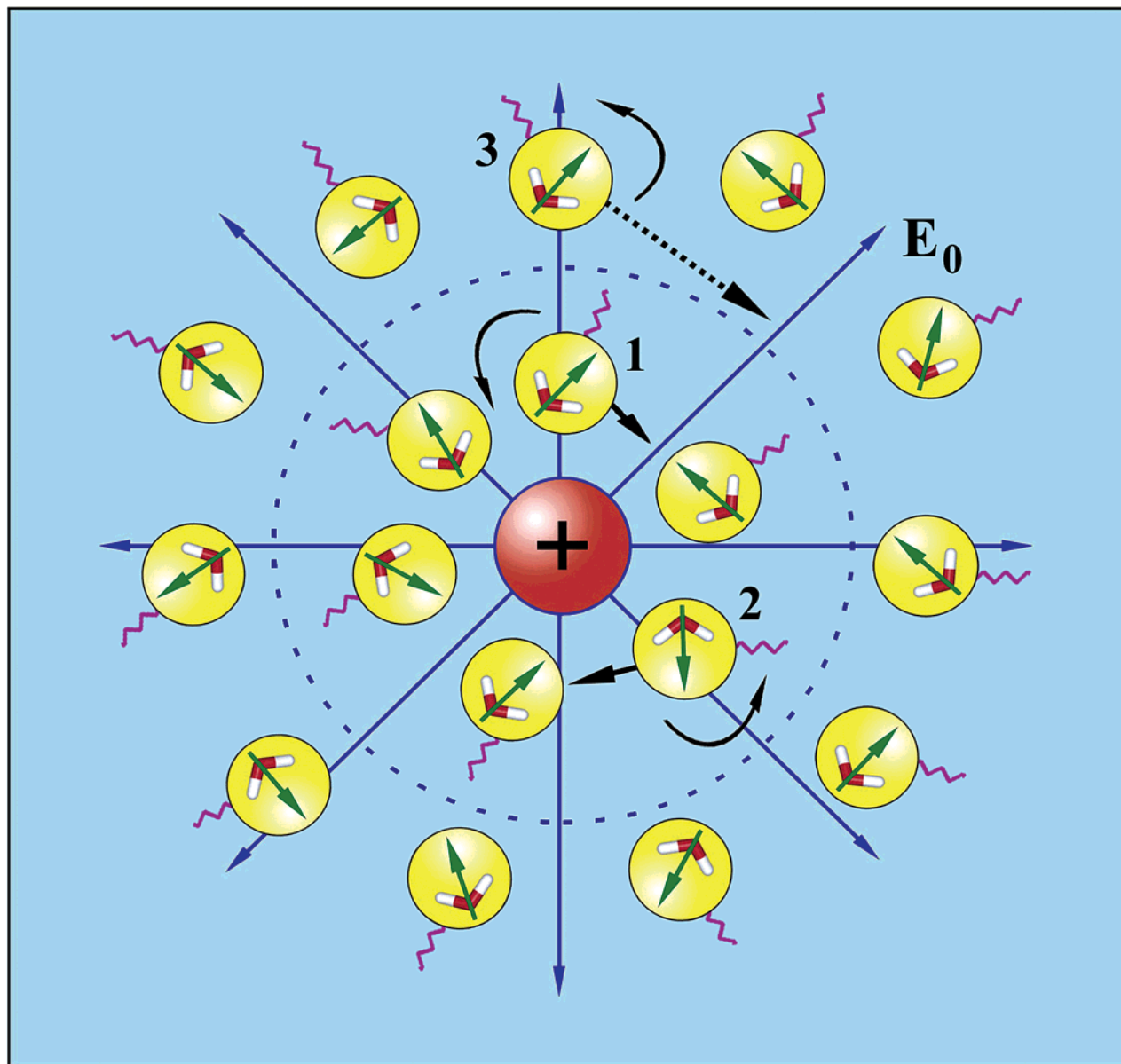


Figure 1. Schematic illustration of solvation of an ion (or dipole) by water. The neighboring molecules (numbered 1 and 2) can either rotate or translate to attain the minimum energy configuration. The field is shown as E_0 . The springs connected to the molecules are meant to denote hydrogen bonding.

where $\mu(\Omega)$ is the dipole moment vector of a molecule at position \mathbf{r} , and $\rho(\mathbf{r},\Omega,t)$ is the position, orientation, and time-dependent density. Therefore, the time dependence of the solvation energy is determined by the time dependence of polarization that is in turn determined by the time dependence of the density. If the perturbation due to the probe on dynamics of bulk water is negligible, then the time dependence of polarization is dictated by the natural dynamics of the liquid.

The theoretical analysis of the time-dependent density is usually carried out by using a molecular hydrodynamic approach that is based on the basic conservation (density, momentum, and energy) laws and includes the effects of intermolecular (both spatial and orientational) correlations. The latter provides the free energy surface on which solvation proceeds. The equation of motion of the density involves both orientational and translational motions of the solvent molecules. The details of the theoretical development are available elsewhere;^{15c} here we

shall present a simple physical picture of the observed biphasic solvation dynamics.

Within linear response theory, the solvation time correlation function is directly related to the solvation energy:

$$C(t) = \frac{\langle \delta E(0) \cdot \delta E(t) \rangle}{\langle \delta E^2 \rangle} = \frac{\langle E(t) \rangle - \langle E(\infty) \rangle}{\langle E(0) \rangle - \langle E(\infty) \rangle} \quad (3)$$

where δE is the fluctuation of solvation energy from the average, equilibrium value. Note that the equality in eq 3 indicates the direct relation for the average of the fluctuations over the equilibrium distribution (left) and the nonequilibrium function (right) which relates to observables; without $\langle E(\infty) \rangle$ the correspondence is clear, and $\langle E(\infty) \rangle$ is rigorously the result of the equilibrium term in the numerator and for normalization in the denominator.

The ultrafast component in the solvation time correlation function (see Figure 3, upper part), originates from the initial

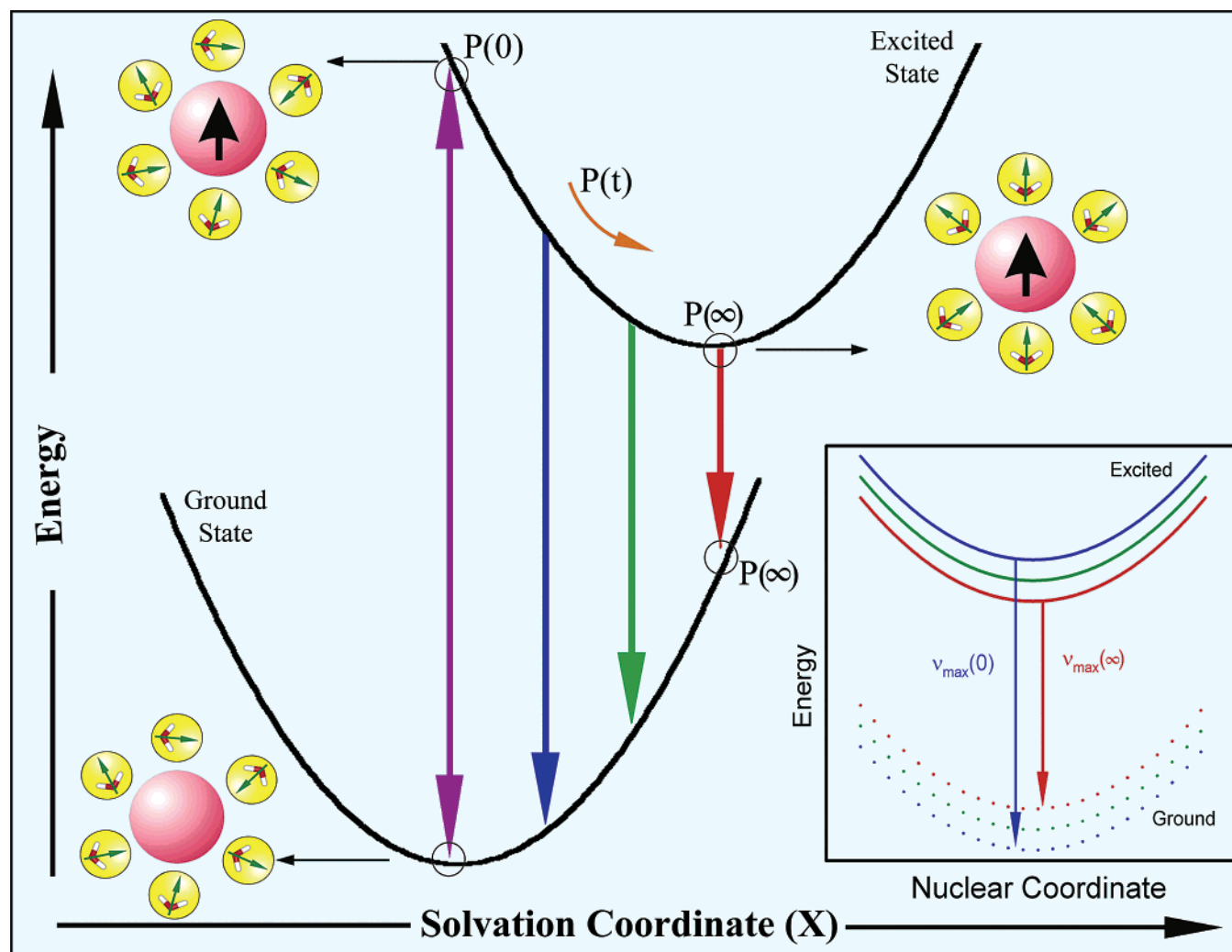


Figure 2. Schematic illustration of the potential energy surfaces involved in solvation dynamics showing the water orientational motions along the solvation coordinate together with instantaneous polarization P . In the inset we show the change in the potential energy along the intramolecular nuclear coordinate. As solvation proceeds the energy of the solute comes down giving rise to a red shift in the fluorescence spectrum. Note the instantaneous P , e.g., $P(\infty)$, on the two connected potentials.

relaxation in the steep collective solvation potential. The collective potential is steep because it involves the total polarization of the system.^{15a,c} This initial relaxation couples mainly to the hindered rotation (that is, libration) and the hindered translation (that is, the intermolecular vibration), which are the available high-frequency modes of the solvent; neither long amplitude rotation nor molecular translation is relevant here. The last part in the decay of the solvation correlation function involves larger amplitude rotational and translational motions of the nearest neighbor molecules in the first solvation shell. In the intermediate time, one gets contributions from the moderately damped rotational motions of water molecules. In a sense, with the above description one recovers the famous Onsager's "inverse snow-ball" picture of solvation.¹⁷

A simple but fairly accurate way to describe the slower part of solvation dynamics (that involves rearrangement of the solvent molecules which are the nearest neighbors of the probe) is to use a wave-vector-dependent relaxation time, as is routinely used in the description of neutron scattering experiments. For slow relaxation, one can use a Smoluchowski–Vlasov-type kinetic equations of motion to describe the rotational and translational motion of water molecules.¹⁸ The following

expression for the k -dependent longitudinal polarization relaxation time:^{15c}

$$\frac{1}{\tau_L^{\text{bulk}}(k)} = 2D_R f(k) \left[1 + \frac{D_T k^2}{2D_R} \right] \quad (4)$$

Here D_R and D_T are the rotational and translational diffusion coefficients, and $f(k)$ is a force constant which describes orientational correlation among the water molecules at wave-vector k . At large values that correspond to the distance of nearest-neighbor separation, $f(k) \cong 1.0$ – 1.5 . At small values ($k \approx 0$), the relaxation time goes over to the standard form of the longitudinal relaxation time.

The above expression (equation 4) reproduces the observed slow decay with time constant of about 1 ps. We take the following values for water:^{19,20} $D_R = 2.2 \times 10^{11} \text{ s}^{-1}$, $D_T = 2.5 \times 10^{-5} \text{ cm}^2/\text{s}$, $f(k) \approx 1$, and $k \cong 2\pi/L$, where L is a measure of the separation length between the solute and the solvent; $L \approx 1.5\sigma$, where σ is the diameter of water molecule (2.8 Å). These values give about 1 ps for τ_L^{bulk} . Varying the range for the parameters, we obtained 0.6–2 ps which still in the range of solvation time scale. Actually, the above good agreement is

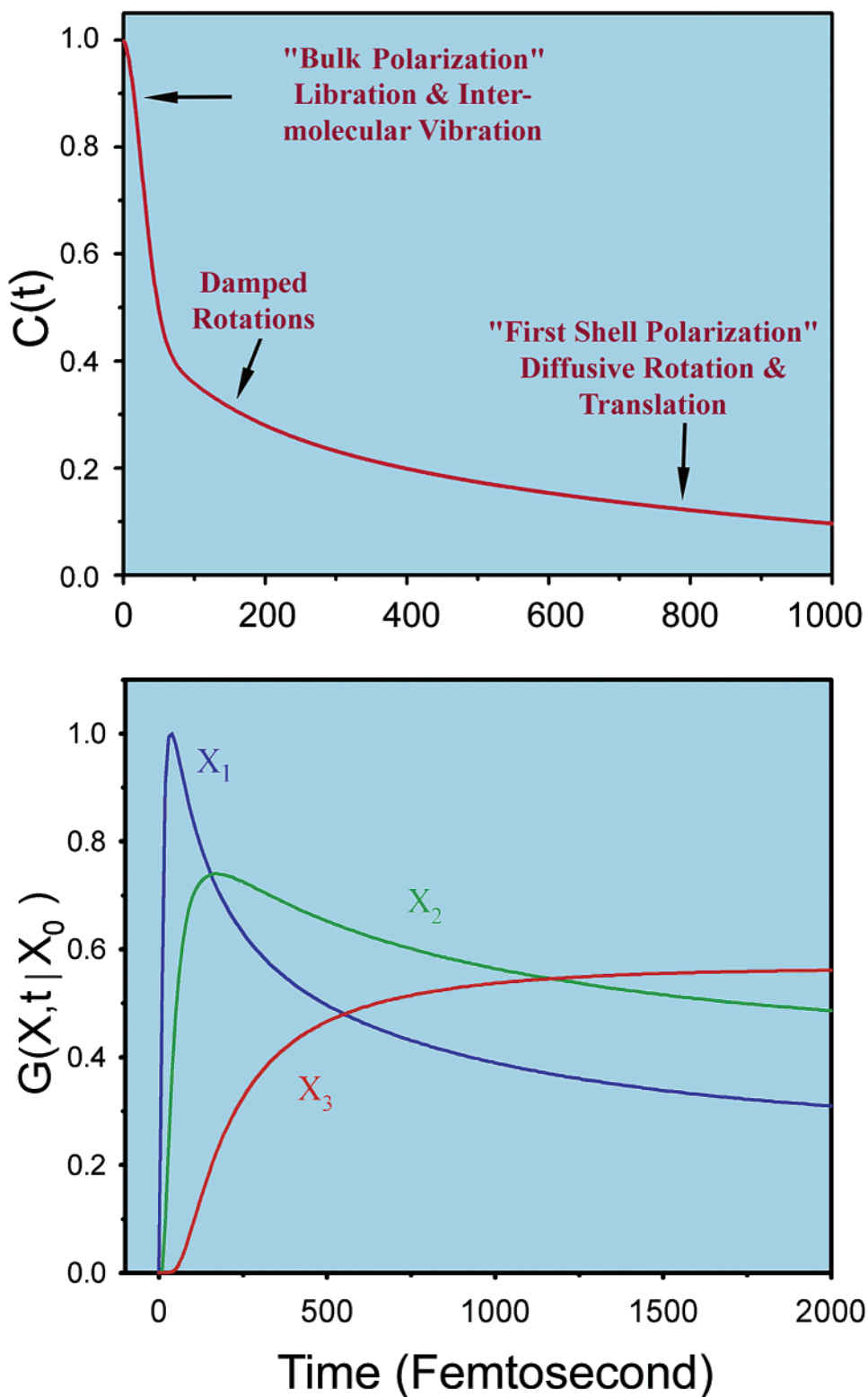


Figure 3. (top) A typical solvation time correlation function for water is shown here. The time correlation function exhibits three distinct regions: the initial ultrafast decay, an intermediate decay of about 200 fs and the last slow decay with time constant of 1 ps. The physical origin of each region is indicated on the plot itself; see text. (bottom) Green's function $G(X,t|X_0)$ for population relaxation along the solvation coordinate X is plotted against time in femtosecond. In G , X_0 is the initial position at $t = 0$. This figure shows the position and time dependence of the population, fluorescence intensity. At early times (when the population is at X_1), there is an ultrafast rise followed by an ultrafast decay. At intermediate times (when the population is at X_2) there is a rise followed by a slow decay as shown by the green line. At long times when the population is nearly relaxed (position X_3 , red line) we see only a rise.

a bit surprising because one expects some perturbation caused by the transport near the solute.

From the behavior of the correlation function of hydration and the above estimate, the picture is clear. The slowest time

constant is about 1 ps which is determined by the individual rotational and translational motions of the molecules in the "first solvation shell" nearly close to the probe. The femtosecond component is dominated by the high-

frequency-hindered rotational and translational (vibration)^{16,21} polarization.

Figure 2 shows a schematic of the solvation potential and the orientational motions for the water molecules involved. From the shape of the potential, it can be seen that the transient behavior for the population during solvation should be a decay function on the blue edge of the spectrum and a rise function on the red edge. These wavelength-dependent features can be explained nicely within a generalized model of relaxation in which a Gaussian wave packet relaxes on a harmonic surface. The relaxation is nonexponential and a Green's function can describe the approach of the wave packet along the solvation coordinate X to its equilibrium value. For the general non-Markovian case it is given by²²

$$G(X,t|X_0) = \frac{1}{\sqrt{2\pi\langle X^2 \rangle [1 - C^2(t)]}} \exp \left[-\frac{[X - X_0 C(t)]^2}{2\langle X^2 \rangle [1 - C^2(t)]} \right] \quad (5)$$

where $\langle X^2 \rangle$ is the equilibrium mean-square fluctuation of the polarization coordinate in the excited-state surface and X_0 is the initial value of the packet on the solvation coordinate.

Equation 5 describes the motion of the wave packet (polarization density) beginning at $t = 0$ (X_0) as a delta function and according to the solvation time correlation function. As $t \rightarrow \infty$, $C(t) \rightarrow 0$ and we recover the standard Gaussian distribution. At early times ($t \rightarrow 0$), the exponential is large, so the decay is ultrafast, but at long times, the relaxation slows down, ultimately to appear as a rise. In Figure 3 (bottom), we present calculations of $G(X,t|X_0)$ at different positions along the solvation coordinate: a decay at X_1 and X_2 , but with different time constants, and a rise at X_3 , as demonstrated experimentally in the coming section.

(B) Experimental: Tryptophan in Bulk Water, a Case Study. Time-resolved fluorescence studies have provided very detailed experimental information about the dynamics of solvation. In particular, with the time resolution of the fluorescence frequency up-conversion method, it has been possible to monitor solvation dynamics by following the evolution of the emission spectrum of a chromophore in solution on the time scale in which solvent relaxation occurs.^{21a} The shift in the chromophore's emission frequency (peak) which accompanies the solvent relaxation is then a measure of the dynamics of solvation. From eq 3 we can define $C(t)$ in terms of observables:

$$C(t) = \frac{\nu(t) - \nu(\infty)}{\nu(0) - \nu(\infty)} \quad (6)$$

where $\nu(t)$ is the emission maximum (in wavenumbers) at time t . As noted in Figure 2, the polarization experienced at a given time is the result of the switched-on field (excited state). Note that in general we must consider the two potentials, excited and ground, and the two coordinates of the probe: intramolecular nuclear motion and that of solvation (Figure 2 and its inset). It is the instantaneous intramolecular Franck-Condon transition that keeps the solvent polarization (see, e.g., $P(\infty)$ in Figure 2) the same in both these states and makes the energy difference between surfaces reflect the behavior of the time-dependent polarization and solvation.

Studies with sub-100 fs time resolution have observed all the time scales involved in bulk water solvation: from the ultrafast features, which take place in a few tens of femtoseconds to the slower parts which occur within 1 ps.^{16,23} Recently, the indole side chain of the amino acid tryptophan (Trp) has been

characterized as an appropriate probe for solvation.^{24,25} The importance of tryptophan in solvation studies is that it can be used to examine the dynamics in a specific location of a protein surface tryptophan which is an integral part of the native state. The indole aromatic ring system in the near UV region has two overlapping electronic transitions, 1L_a and 1L_b , with nearly perpendicular transition dipole moments.²⁶ The 1L_b state has been identified as the emitting state in nonpolar environments, while the 1L_a state is the emitting state in polar media and has a large dipole moment.

Recent anisotropy measurements from fs fluorescence up-conversion have determined that the internal conversion process of the fluorescent state in water (1L_a) actually takes place in less than 100 fs.^{24,25} This finding contrasts a previous conclusion²⁷ which had indicated that such electronic-mixing dynamics occurs on the time scale of 1 to 2 ps, and hence mask the solvation dynamics occurring on this time scale. With the sub-100 fs formation of the solvation-sensitive 1L_a state, the internal conversion dynamics can be considered to be well-separated from solvation dynamics which occur on the hundreds of femtoseconds and up to 1 ps.

Figure 4 shows the results of fluorescence up-conversion experiments of tryptophan in aqueous solution.¹⁰ The upper section of the figure depicts population transients at three representative wavelengths and the lower part gives the corresponding spectral evolution (inset) and the hydration (solvation) correlation function $C(t)$. The solvation dynamics observed were fitted to a biexponential decay, with a time constant of 180 fs (20%) and another of 1.1 ps (80%); the earliest <50 fs component is not resolved. The net dynamic spectral shift is 2350 cm^{-1} . Clearly, these experiments are resolving the slower diffusive part of the solvation dynamics following the large dipole increase ($\sim 6 \text{ D}^{26}$) of the indole chromophore upon the sub-100 fs formation of the fluorescing 1L_a state (up-conversion experiments of tryptophan in alcohols also produced the corresponding typical solvation features of these liquids, as shown in this laboratory and elsewhere²⁴). A set of these results give the correlation function shown in Figure 4. From our reported results in Figure 4, the behavior of the population change and the correlation function are entirely consistent with the theoretical analysis of Figure 3.

III. Dynamics of Protein Hydration: Theory

Solvation dynamics of an external probe located at the surface or in hydrophobic pockets/clefts of a protein is rather complex because it derives contributions from spatial and temporal inhomogeneities. Experiments have shown, using coumarin²⁸ or eosin²⁹ as an extrinsic dye probe, that a multiphasic behavior is present but still with short and long time components. In one such studies, the observed relaxation (for coumarin) is attributed entirely to a hydrophobic pocket in the solvent-inaccessible region.²⁸ For the other probe (eosin)²⁹ the X-ray structure (see below, section V) indicates that it is in a hydrophobic pocket. Even with a natural probe,¹⁰ we must consider the different contributions to solvation, the protein molecule, the water in the hydration shell and the bulk water, but we can eliminate the inhomogeneity in bindings and the local changes due to a foreign probe.

In the following we consider the different processes involved in protein hydration, with the following questions in mind: What is the microscopic origin of the long-time solvation dynamics? If the slow solvation arises from the hydration layer, then why does the 1 ps component continue to persist? What is the residence time, and its distribution, and why does it affect the friction by translational and rotational motions?

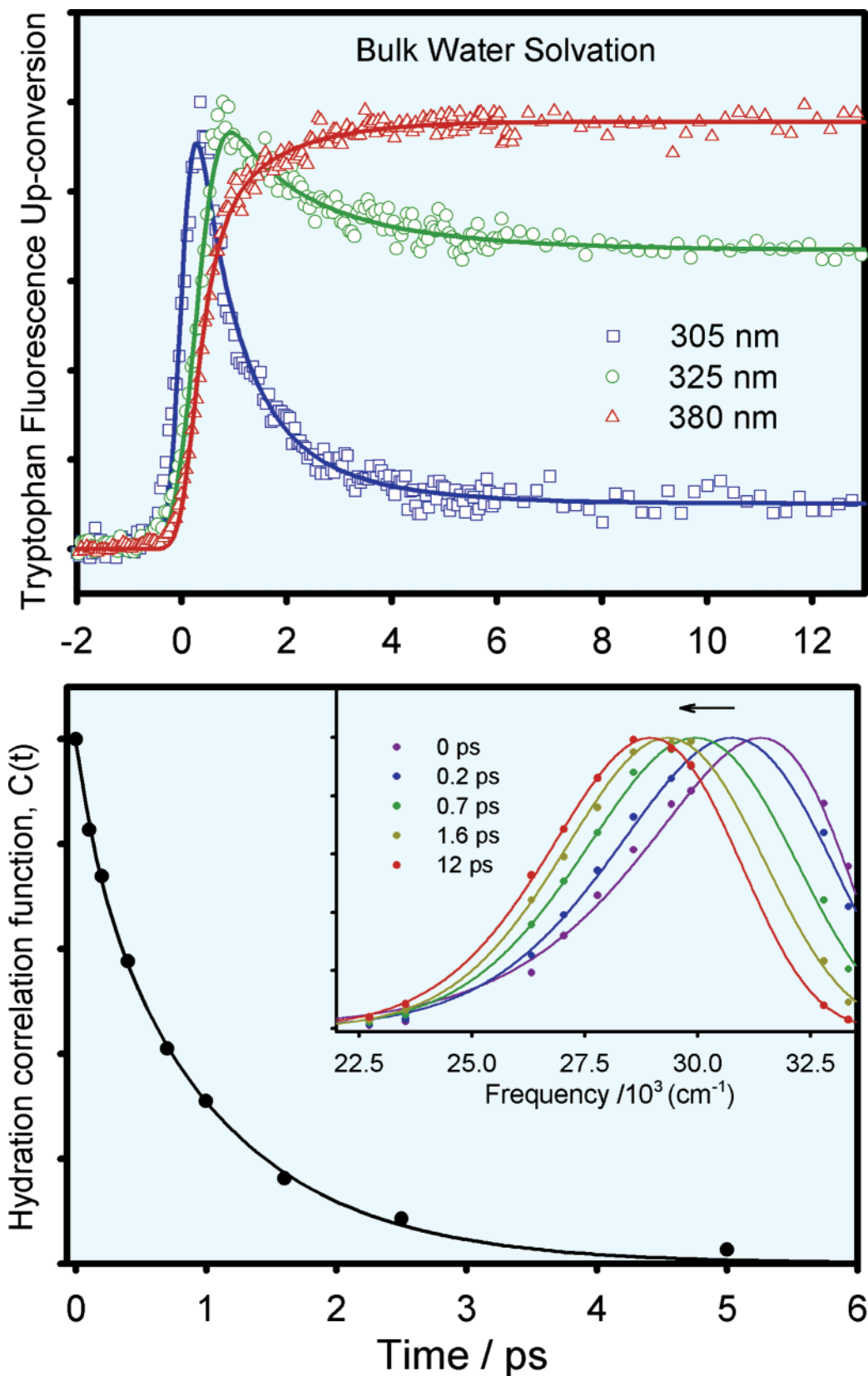


Figure 4. Femtosecond resolved fluorescence (upper) and solvent response function (lower) obtained for aqueous tryptophan solutions with an excitation wavelength of 288 nm. The results give the decay of the hydration correlation function in bulk water. The insert shows the normalized spectral evolution at five delay points. The evolution with time clearly shows the origin of the observed decay (see, e.g., the point at 32.5) and the rise (see, e.g., the point at 26). The magnitude of the decay or rise component, relative to the relaxed component, depends on the magnitude of the net shift and the lifetime of the relaxed state. The spectra shown are normalized, but, in general, they may change in amplitude with time because of Franck–Condon factors; if the lifetime of the relaxed state is too short then this decrease is serious and a build up may not be observed, as discussed in text for other systems.

(A) Polarization Relaxation of Hydration Layer. Both the structure and the dynamics of water molecules in this layer are influenced by the interactions with the protein, especially with the polar and charged groups at the surface. Water molecules form hydrogen bonds with these groups and the strength of this bonding vary from group to group, as already discussed in the Introduction. When strongly hydrogen bonded to the protein, the water molecules cannot contribute to solvation dynamics because they can neither rotate nor translate. But the hydrogen bonding is transient, and there is a dynamic equilibrium between the free and the bound water molecules. The physical process is shown pictorially in Figure 5 (upper part). The potential of mean force can be represented by a double well structure, as shown in Figure 5 (bottom), to symbolize the process of bond breaking and bond forming. This figure shows an effective potential energy of a water molecule as a function of distance from the protein surface. Here we have assumed that the transition from the bound to the *quasi-free* state occurs along the distance from the protein surface which is taken to be the primary reaction coordinate of this event.

However, hydrogen bonds can also break via rotation. In fact, in the limit of small binding energy, this mode of interconversion between the free and the bound states could be more efficient. When the binding energy is large (compared to $k_B T$, where k_B is Boltzmann's constant and T the temperature), then this mechanism is not as efficient because the majority of bonds broken by rotation can re-form immediately. Thus, the molecule needs to be physically removed from the position next to the protein surface to a certain distance away to be considered as free. The kinetic model we employ is general and independent of the potential energy surface. The details of the bond-breaking mechanism enters only through the rates of interconversion, as discussed below.

The theoretical description requires solution of two coupled reaction–diffusion equations, discussed in Appendix I, which include the dynamic equilibrium. Two rate constants, k_{bf} and k_{fb} , are introduced to describe the transition from bound (to the surface) to free (from the surface) and the reverse, respectively: bound \rightleftharpoons free (rotating and translating). As shown in Appendix I, the resulting equations can be solved for the polarization to find two wave-vector-dependent relaxation times (τ_{\pm}):

$$\tau_{\pm}^{-1} = \frac{1}{2} \left[-A \pm \sqrt{A^2 - \frac{4k_{bf}}{\tau_s^{\text{bulk}}(k)}} \right] \quad (7)$$

where $A = [\tau_s^{\text{bulk}}(k)]^{-1} + k_{fb} + k_{bf}$. Here, $\tau_s^{\text{bulk}}(k)$ is the wave-vector-dependent bulk solvation time, given by eq 4 (with now $f(k) = 1$). These rates depend on the binding energy and will vary from site to site.

The above expression of solvation times gives simple results in the limit of large activation barrier between the bound and free states. This is because $(\tau_s^{\text{bulk}}(k))^{-1}$ is close to 10^{12} s^{-1} and the transition rates, k_{bf} and k_{fb} , are expected to be smaller. In this case, the time constants are given by

$$\tau_{\text{fast}} \equiv |\tau_{-}| \approx \tau_s^{\text{bulk}} \quad (8a)$$

$$\tau_{\text{slow}} \equiv |\tau_{+}| \approx k_{bf}^{-1} \quad (8b)$$

In the same limit of large activation energy separating the bound state from the free one, the residence time of the bound water molecules is given essentially by k_{bf}^{-1} , which is in the range of tens of picoseconds. Even if k_{fb} is significant one can show the

direct relationships given above, modified by a bifurcation factor. The expressions of the rates are given below.

(B) Orientational Relaxation. Orientational relaxation of water molecules in the hydration shell gets modified because of the dynamic equilibrium between free and bound molecules. The logic runs as follows. First note that the orientational diffusion ($D_R = 2.2 \times 10^{11} \text{ s}^{-1}$)¹⁹ relaxation of the water molecules in the bulk is largely single exponential, with a time constant of about 2.3 ps. The orientational relaxation of *quasi-free* water molecules in the hydration shell of a protein is not expected to slow appreciably. Simulations have confirmed this fact;³⁰ simulations also show the existence of a very slow component for those water molecules which remain bound at the surface of a micelle.³¹ This slow component, which could last for hundreds of picoseconds, is a clear signature of bound water molecules.

We can derive an expression for this slow relaxation by using the same dynamic exchange model described above. The model is to consider the rotation of the *quasi-free* water molecules within the hydration layer. Thus, the mode of decay of the orientational correlation by escape to the bulk is deliberately not considered here because our focus is on the dynamics inside the hydration shell. The details of the model will be discussed elsewhere—here we present a somewhat simpler version. The starting point is the similar kind of coupled reaction–diffusion equations, discussed in Appendix I, which can be solved to obtain the two rate constants k_{\pm} given by

$$k_{\pm} = \frac{1}{2} [-B \pm \sqrt{B^2 - 8D_R k_{bf}}] \quad (9)$$

with $B = 2D_R + k_{fb} + k_{bf}$. This equation is similar to that of eq 7, limiting solvation by only rotational diffusion, i.e., $\tau_s^{\text{bulk}} = 1/(2D_R)$ (see eq 4). In the limit where the rate of conversion from bound to free becomes very small, large barrier, the above expression further simplifies and the two rates are given by $2D_R$ and k_{bf} . Thus, while one time constant remains fast, of the order of 2–3 ps, the other one becomes much slower k_{bf}^{-1} , the rate determined by the binding energy. We note that the fast component of solvation could become even shorter if translational diffusion is included, eq 7, as discussed below.

The above result has some important ramifications. Dielectric relaxation measurements of aqueous protein solutions often find a slow nanosecond component, which is usually attributed, at least partly, to the orientational relaxation of the water molecules in the hydration shell. By using the above expression, we can now put an upper bound on the time constant from knowledge of the distribution of binding energy. This theory predicts that the relaxation should be in the range of 20–300 ps. Therefore, the ~ 1 –10 ns component reported⁹ in the dielectric relaxation literature should be primarily due to the side chain (and protein) motions and nearly static water, not from the dominant dynamics of biological water. The theory thus predicts a biexponential decay for a given binding energy. However, there is a distribution of binding energies. This can lead to highly nonexponential orientational dynamics and can explain the stretched exponential decay of orientational relaxation observed recently in MD simulations of proteins¹⁴ and micelles.³¹ We now consider expressions for k_{bf} and k_{fb} , and the residence time.

(C) Residence times and Rates. We first estimate the residence time by using the following well-known expression for translational motion:

$$\tau_{\text{res}} = L_H^2 / 6D_{\perp} \quad (10)$$

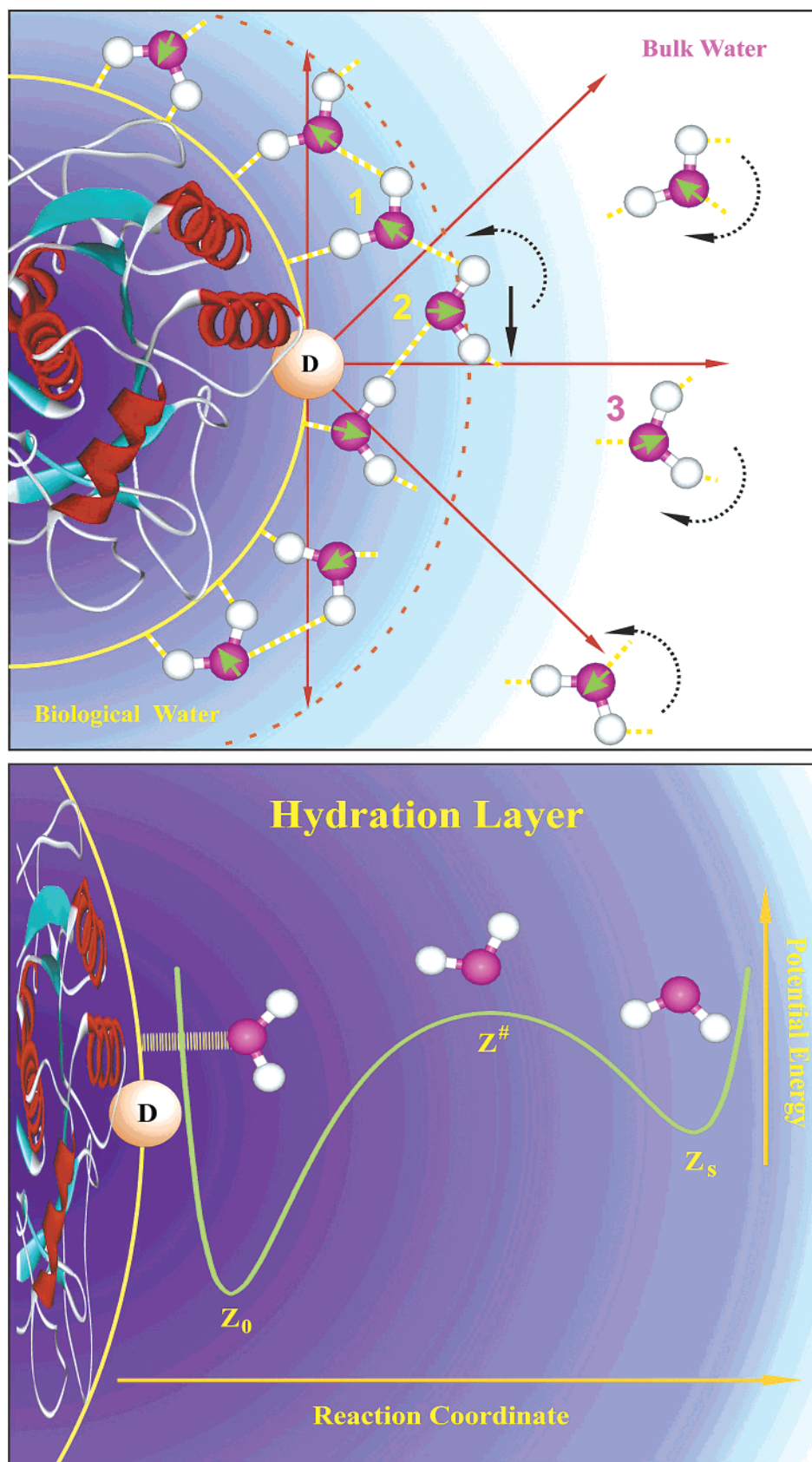


Figure 5. An illustration of the dynamic equilibrium in the hydration layer of a protein, with bound (1) *quasi-free* (2) and free water molecules (3). The potential for the exchange is shown in the lower part, see text.

where τ_{res} is the time taken to cross the layer. D_{\perp} is the diffusion in the perpendicular (to the protein surface) direction and L_H is the width (or, thickness) of the biological layer (note the factor 6 here, not 2, because we are still in 3 dimensions). L_H is

typically 4 Å, and D_{\perp} is to be calculated as follows. In the bulk, D_{\perp} is $1/3 D_{\text{bulk}}$. Typical value of D_{bulk} is 2.5×10^{-5} cm²/s.²⁰ However, in the hydration shell, both the parallel and perpendicular components of the diffusion coefficient decrease, the

perpendicular one being more affected. It is reasonable to assume that D_{\perp} is somewhat less than the bulk value. Thus we obtain an estimate of τ_{res} of 32 ps (for $D_{\perp}=1/3D_{\text{bulk}}$) or longer.

In reality, the residence time of water in the biological layer is determined by the nature of the interaction with the surface. Let us assume that $V_i(z)$ denotes the reduced energy of interaction of a water molecule with the site i on the protein surface; z is the direction perpendicular to the surface. $V_i(z)$ will have a minimum at $z \approx 3-3.5 \text{ \AA}$. At smaller distances from the surface, the energy should rise sharply. The potential is shown schematically in Figure 5. We can obtain a closed form expression for the escape time by calculating the mean first passage time which is obtained by using the method of images.³²

The physical picture behind this derivation is simple. The diffusing molecule is modeled as a random walker. The boundary on the bulk side is an absorbing wall (or barrier), while the protein surface is modeled as a reflecting barrier. The water molecule executes a random walk under the influence of the potential $V_i(z)$. The equation of motion is given by a Smoluchowski equation.³² The first passage time can be obtained from the adjoint of this equation. An elegant description of the method is given in ref 32. The final expression of the mean first passage time is given by

$$T(z_0) = \frac{1}{D_T} \int_{z_0}^{z_s} dy e^{\beta V_i(y)} \int_b^y dx e^{-\beta V_i(x)} \quad (11)$$

where b is a position of smaller values than z_0 and $\beta = 1/(k_B T)$. $T(z_0)$ has a dependence on the initial position z_0 and also on the hydrogen bond strength, through $V_i(z)$. Thus, this $T(z_0)$ will have a distribution. The average residence time is given by the following double averaging,

$$\langle \tau_{\text{res}} \rangle = \langle\langle T(z_0) \rangle\rangle = \int dz_0 P(z_0) \int d\epsilon P(\epsilon) T(z_0) \quad (12)$$

where $P(z_0)$ is the initial population distribution in the potential well and $P(\epsilon)$ is the distribution of the hydrogen bond energy with binding energy ϵ . One can even include the effects of hydrophobic interaction by including a repulsive surface. Note that the above expression for the residence time is general.

Now, if we make the assumption that the interconversion between the bound and *quasi-free* molecules occur on the same potential energy surface, then the same procedure as described above can be used to obtain expressions for the rate constants k_{bf} and k_{fb} . The final expression for k_{bf} is

$$k_{\text{bf}} = \frac{D_T}{\int_{z_0}^{z^{\#}} dy e^{\beta V_i(y)} \int_b^y dx e^{-\beta V_i(x)}} \quad (13)$$

Note that the upper limit of integration in the first integral is different from that in eq 11, because the bond breaks when the coordinate reaches the position $z^{\#}$. The expression for k_{fb} is obtained by reversing the initial and final states.

To make quantitative estimates of the various quantities, we need to assume a potential energy $V_i(z)$ for the transition from bound to free water. As a first approximation, one can assume that this is given by a double Morse potential

$$V_i(z) = E_b^i [1 - e^{-(z-z_b)/\lambda_b}]^2 - E_b + E_b [1 - e^{-(z-z_b)/\lambda_b}]^2 - E_b' \quad (14)$$

where E_b^i is the hydrogen bond energy with i th polar or ionic

group of the protein amino acid. E_b' is the hydrogen bond energy of the *quasi-free* molecules. The length parameters λ_b and λ_b' are obtained by imposing conditions of continuity of the potential and its first derivative. As already mentioned, the presence of a second shallow minimum is suggested by a second peak in the radial distribution function and is also expected on theoretical grounds.

With the above representation of the reaction potential energy, we can now find an estimate of the binding energy responsible for the slow solvation time. By using eq 13, numerical calculations give a value of 2.3 kcal/mol for SC and 1.2 kcal/mol for Monellin in order to account for the observed, respectively, 38 and 16 ps time constants. Because of the existence of binding sites of different energies on the protein surface it is convenient to discuss dynamics in terms of a distribution of residence times. Once an expression of the residence time is available, it is easy to translate the distribution of binding energy to the distribution of residence times. This is simple because we can calculate the residence time at each energy, eq 11.

In an extreme limit one may consider an exponential distribution of binding energies ϵ on the protein surface, i.e.,

$$P(\epsilon) = (1/\epsilon_c) \exp(-\epsilon/\epsilon_c) \quad (15)$$

where ϵ_c is the single energy parameter that quantifies the distribution. Therefore, the distribution of residence time is a function of both ϵ and ϵ_c . It is now straightforward to obtain the distribution of residence times, given an ϵ_c . In Figure 6 we show a calculation of the distribution of residence times. Note the slow tail at long times which is expected and has already been observed in simulations. In the lower part of the same figure we show a corresponding solvation time correlation function where the contributions from the two different time scales are indicated. A more realistic distribution is that involving at least a bimodal distribution, that which has a peak near $\epsilon \sim 0$ and another at a shifted value for ϵ_c . As such the sum of the two defines the *hydrophobic* and *hydrophilic* interaction regions with total $P = \alpha P_1 + \beta P_2$. For the latter bimodal distribution, we show $C(t)$ in Figure 6, which indeed is robust in its behavior.

(D) Solvation and Residence Time. Because the residence time is a measure of the mobility of the water molecules, one intuitively expects a relationship between solvation dynamics and the residence time of a water molecule in the hydration layer. The separation in time scales allows us to obtain such relationship for the two major components of hydration, for the ultrafast ~ 1 ps component and for the slow 20–50 ps component. The time constant for the fast part of solvation is given by eq 8a, and earlier we considered only rotational diffusion, eq 9. We now consider the additional translational diffusion, $\tau_{\text{res}} = L_H^2/(6D_{\perp})$, which is given in eq 10. We now combine eq 4 and 8a and use eq 10 to eliminate $D_{\perp}(=D_T/3)$, yielding

$$\tau_{\text{solv}}^{-1} = \tau_{\text{rot}}^{-1} + \left(\frac{1}{2} L_H^2 k^2\right) \tau_{\text{res}}^{-1} \quad (16)$$

where τ_{solv} is the solvation time (ultrafast part) of the hydration shell, $\tau_{\text{rot}} = (2D_R)^{-1}$ and $k \approx 2\pi/(1.5\sigma) = 4.19/\sigma \text{ cm}^{-1}$.

According to this linear relationship, the slope in Figure 6 (upper part, inset) gives $\approx 9(L_H/\sigma)^2$, square of the ratio of the thickness of the layer to the molecular water diameter times 9. This relation 16 for the ultrafast part of solvation, which is determined by the motion of free or *quasi-free* water molecules,

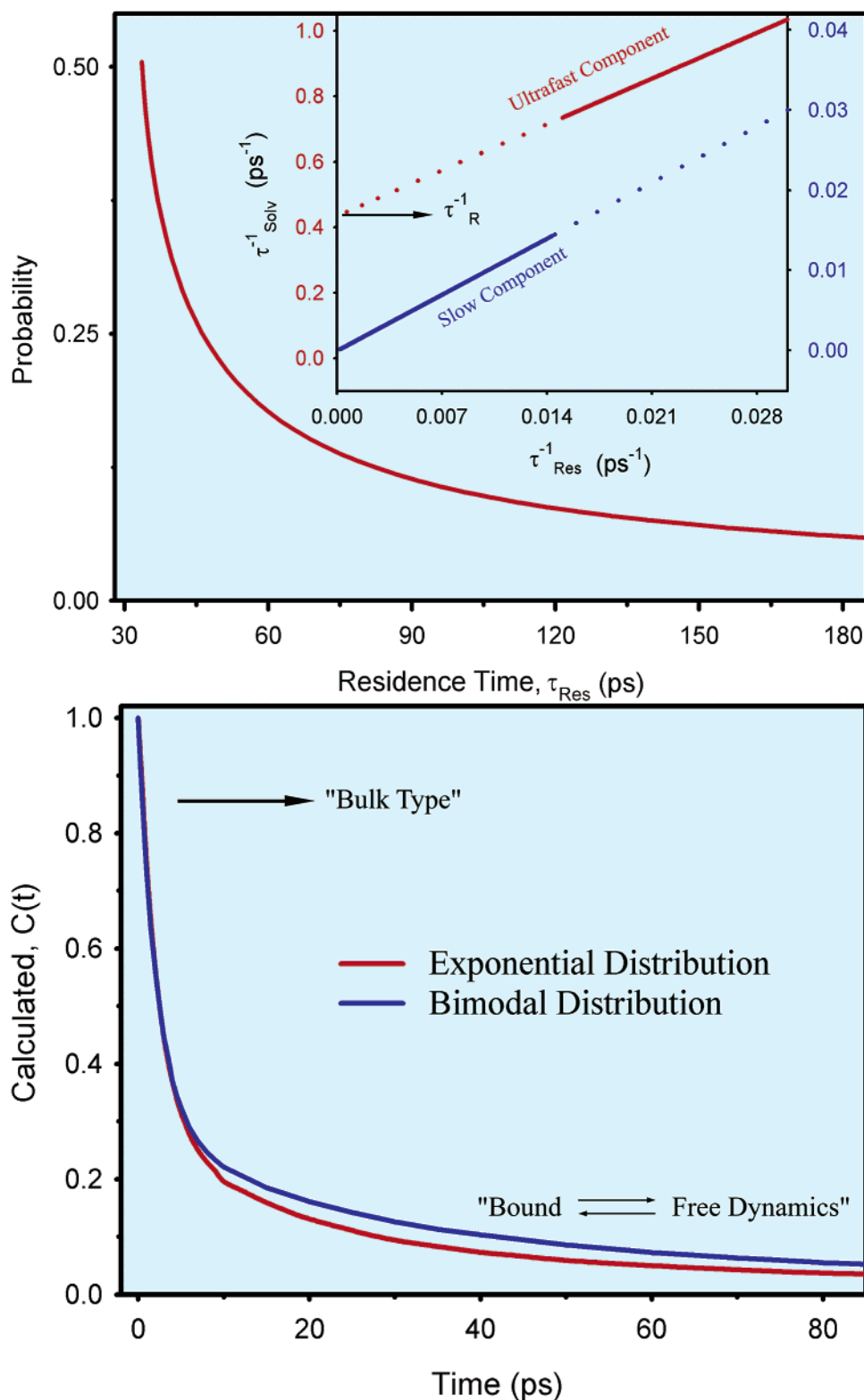


Figure 6. The calculated probability distribution for the residence time (upper) and solvation time correlation function $C(t)$ (lower). Two different types of distribution are plotted: A single-exponential function with an average binding energy of $\epsilon_c = 2k_B T$, and a bimodal distribution with peak average values $\epsilon_c(1) = 0.5k_B T$ and $\epsilon_c(2) = 3k_B T$ with $P = 0.3P_1 + 0.7P_2$. In the inset of the upper part we plot the relationship between the residence time and the solvation time describing the linear behavior and approximate validity regions.

shows that the contribution to the solvation rate is from the typically bulk-type rotational diffusion in addition to the contribution from translational diffusion; when the latter reaches the bulk value ($D_T = 2.5 \times 10^{-5}$ cm²/s), which reflects the dynamics of “free molecules”, the solvation time decreases at

most by a factor of ~ 2.3 , indicating that the ultrafast component remains that of bulk-type.

On the other hand, for the slow component of solvation (20–50 ps), which reflects the dynamics of bound water molecules, the residence time is given by the inverse of the rate of transition

from the bound to the free state, eq 8b; that is,

$$\tau_{\text{res}}^{-1} = k_{\text{bf}} \quad (17)$$

This is an interesting result that shows that the long time component of polar solvation dynamics is equal to the residence time of the water molecules. Again, the deviation for the general case is relatively small, as discussed in section III.A.

IV. Experimental: Femtosecond Protein Hydration Dynamics

In this section we present our studies, with femtosecond resolution, of hydration dynamics at the surfaces of the proteins Subtilisin *Carlsberg* (SC) and Monellin (see Figure 7 for the high-resolution X-ray structures). The protein SC is an enzyme (serine endopeptidase), while Monellin is a plant protein that tastes sweet (50000 times sweeter than ordinary sucrose). Although the biological functions of the proteins are different, both contain only one tryptophan (SC: Trp-113; Monellin: Trp-3 of chain B). These single tryptophan (Trp) residues were used as intrinsic biological probes for the hydration dynamics. The details of the studies can be found elsewhere.^{10,33}

As mentioned above, the main advantage of using the amino acid tryptophan as a hydration probe is that its intrinsic nature rules out the ambiguity about the location of the probe and hence the environmental heterogeneity (spatial averaging). The photophysical properties of Trp and its spectral shift when it is solvated in polar environments has been thoroughly studied. Moreover, the intramolecular processes of Trp occur on the time scale of less than 100 femtoseconds and do not mask solvation dynamics which occur on the one picosecond time scale as detailed in section II.B. By exciting Trp near the lowest vibrational energy we can eliminate complications due to vibrational relaxation and energy redistribution. Finally, the indole chromophore of Trp has a much larger dipole moment in the excited state than in the ground state ($|\Delta\mu| \cong 6 \text{ D}$)²⁶ indicating the near instantaneous switch of a net dipole in polar water.

(A) The Enzyme Protein SC. The hydration correlation function $C(t)$ obtained from fluorescence up-conversion experiments on aqueous solutions of SC is shown in Figure 8 (upper part). A detail description of the procedure to construct $C(t)$ and the time-resolved spectra of the SC has been given elsewhere.¹⁰ The hydration dynamics of the SC protein shows significant differences when compared with the results of Trp in bulk water. In particular, the $C(t)$ decay shows a considerably slower and additional decay component. $C(t)$ of the protein is described by the sum of two exponentials, with $\tau_1 = 800 \text{ fs}$ (61%) and $\tau_2 = 38 \text{ ps}$ (39%); the less than 50 fs component was not resolved. The net dynamic spectral shift is 1440 cm^{-1} . For Trp in bulk water, $C(t)$ longest time constant is $\tau = 1.1 \text{ ps}$.

To measure the local rigidity of the Trp in SC, we studied the fluorescence polarization anisotropy, $r(t)$ (see the inset of the Figure 8, upper part). The behavior of $r(t)$ is not complicated by internal conversion between the 1L_a and 1L_b states of Trp since the $r(0)$ value we observe (0.2) reflects a sub $\sim 100 \text{ fs}$ electronic-state mixing.¹⁰ The anisotropy of Trp in the protein decays by a 55 ps to a constant value of ~ 0.1 (value at 200 ps). This almost constant anisotropy level, which was absent in Trp in bulk water, indicates that the orientational dynamics is significantly restricted when compared with bulk orientational relaxation (35 ps); solvation occurs on an essentially "static" probe.

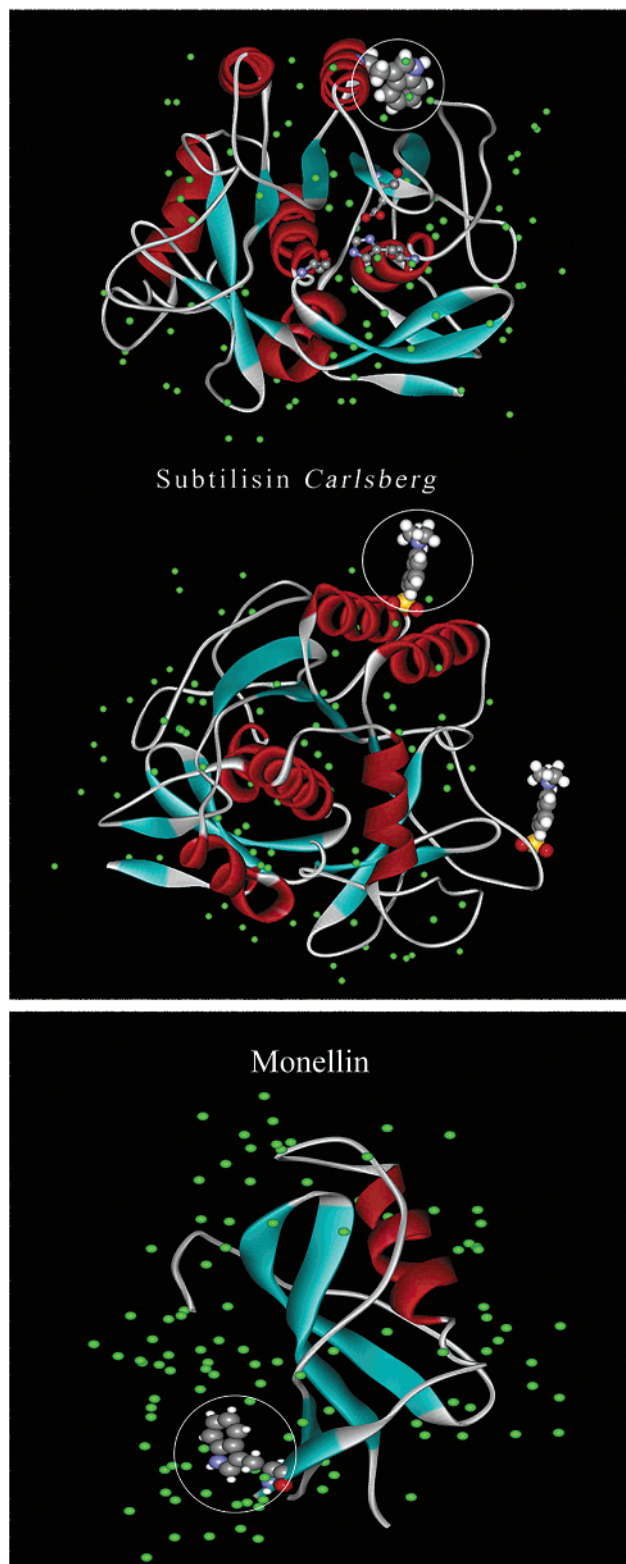


Figure 7. The X-ray structure of the protein Subtilisin *Carlsberg* (SC) (top). The intrinsic probe tryptophan of the protein is highlighted by a circle. In the middle part the extrinsic dye molecule DC attached to the protein SC is shown. Two DC binding sites are highlighted. The lower part shows the X-ray structure of the sweet protein, Monellin monomer. The dimeric structure was downloaded from Protein Data Bank (with the code 4MON) and processed with WEBLAB-VIEWERLITE to show one of the identical monomers, for the sake of clarity. In solution, Monellin exists in the monomeric form.⁴⁷

To estimate the thickness of the hydration layer in the protein surface, we studied the dynamics for a dansyl chromophore that

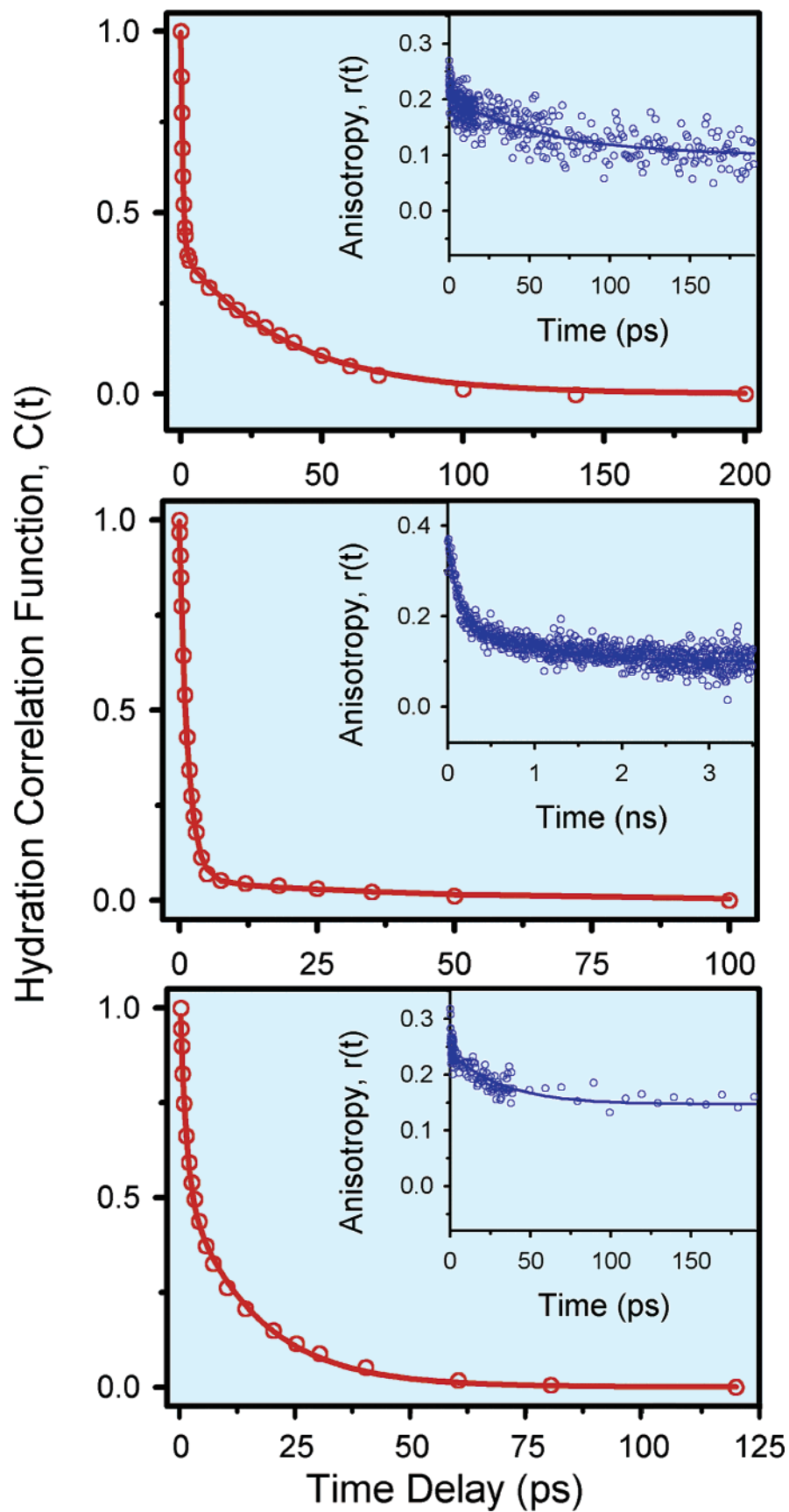


Figure 8. Experimental observations of the hydration for the proteins Subtilisin *Carlsberg* and Monellin. The time evolution of the constructed correlation function is shown for the protein SC (top), the Dansyl bonded SC (middle), and the sweet protein Monellin (bottom). The corresponding time-resolved anisotropy $r(t)$ is given in the inset of each part (for SC and Monellin the anisotropy was measured at 370 nm, and for Dansyl bonded SC, at 510 nm).

is covalently attached to the water-exposed residues, such as lysines and arginines of the protein SC. On the basis of bond lengths, we estimate that the location (~ 7 Å) of the dansyl probe when bound to SC is such that it sees relatively smaller interaction with the protein environment in comparison with bulk water. The constructed $C(t)$ shows (Figure 8, middle part) an ultrafast decay with a time constant of 1.5 ps (94%); a very small amount of spectral shift occurs with a time constant of 40 ps (6%). The near absence of the long decay component (40 ps) indicates that at the separation of ~ 7 Å from the surface of SC the solvent dynamics resemble, to a large extent, those seen in bulk water.

The anisotropy $r(t)$ for the protein in buffer solution is consistent with the binding of the dansyl probe to the protein, not as a free motion in bulk (~ 50 ps in methanol).³⁴ The anisotropy decay (inset of Figure 8, middle part) measurement, from time correlated single photon counting, gives $r(0) \sim 0.4$ and shows two decays, 100 ps (46%) and ~ 1 ns (28%), after which $r(t)$ at $\sim 26\%$ persists for at least 4 ns. The persistence of the $r(t)$ is consistent with the probe being attached to the protein SC, which has a very long rotational relaxation time; the 100 ps component may reflect the restricted motion in a cone.³⁵

The behavior of $C(t)$ for the protein is entirely consistent with the theoretical formulation discussed in section III. The Trp site is probing a dynamical water in the hydration layer with a thickness of less than 7 Å. The ultrafast component, within our time resolution, indicates that we are observing *quasi-free* water molecules of the layer with the contribution of translational diffusion similar to that of the bulk (see eq 16). The long decay component of 38 ps reflects the motion of bound molecules to the surface site, and according to eq 17 gives the bound to free residence time. The overall behavior of $C(t)$ reflects the distribution in residence times, mainly by two types of bonding: 2–3 kcal/mol for the surface bound molecules on our time scale of 38 ps and $\leq k_B T$ kcal/mol for the *free/quasi-free* molecules.

(B) The Sweet Protein Monellin. The single tryptophan residue of the protein Monellin is on the surface and is significantly exposed to the water environment. By following the time-resolved Stokes shift of the emission spectra, we constructed³³ the hydration correlation function $C(t)$, as shown in Figure 8, lower part. The hydration at the surface of the protein gives rise to slower dynamics compared to that in bulk water. The $C(t)$ can be fitted to a biexponential with the time constants 1.3 ps (46%) and 16 ps (54%); the less than 50 fs component is not resolved. The net dynamic spectral shift is 960 cm^{-1} .

The anisotropy $r(t)$ of the Trp confirms a restricted environment around the probe. The $r(0)$ value is 0.24 and $r(t)$ can be fitted by two terms; one is an exponential decay with time constant of 32 ps (37%) and another that is a constant term of ~ 0.15 (63%), which is persistent at least up to 300 ps (inset of Figure 8, lower part). The constant term is consistent with the very slow rotational relaxation of the probe as it is anchored with the protein Monellin, while the faster one may reflect the restricted motion in a cone.³⁵

With $C(t)$ and $r(t)$ for Monellin we arrive at similar conclusions to that of the SC protein, except for the time scales. The ultrafast component is somewhat longer than that of bulk water and this is consistent with a contribution from rotational and translational diffusion of *quasi-free* water (note that the effect of k in eq 16 should also be considered). The long time component of 16 ps is a residence time for a typical binding

energy of 1.2 kcal/mol. The relative size of the protein (SC is 3 times larger than Monellin) and the degree of exposure of Trp are factors that we shall consider in future MD simulations.

(C) Denatured Monellin. We have discussed how the observed dynamics of the solvent are directly dictated by the hydration sites near the tryptophan moiety at the surface of fully folded protein. It is expected that a disruption of this globular landscape should lead to important changes in the hydration dynamics, and if it is significant, it provides an opportunity to elucidate dynamics of the nonnative state. Under sufficiently denaturing conditions, the macromolecule unfolds to a statistical random coil in which the probing chromophore samples a wide set of environments varying from those which are exposed to bulk, hydrophobic groups, and the charged groups of amino acids.

To explore such possibilities, we have studied solvation dynamics of Monellin denatured with 6 molar guanidine hydrochloride (GndHCl).³³ At this concentration, the protein is considered to exist in the random coil state.³⁶ Denaturation leads to a significant red-shift of the steady-state fluorescence spectrum of the protein, from 342 nm in the native state to 352 nm in the 6 M GndHCl solution. This change is associated with the disruption of the folded state of the protein.

In the 6 M GndHCl solution, $C(t)$ of Monellin is completely altered from that of the native state in buffer solution (see Figure 9). The $C(t)$ in this case shows a “biexponential” decay with $\tau_1 = 3.5$ ps (72%) and $\tau_2 = 56$ ps (28%). The net dynamic spectral shift is 1140 cm^{-1} . The changes with respect to the native-state solvation can be summarized as follows: (1) There is an increase in the time constant of the early dynamics from the native case of 1.3 ps. (2) The contribution of the fast part to the total shift is significantly larger, going from 46% in the native to 72%. (3) The slow component of the spectral shift is now more than 3-fold increased from the slow component in the native protein case of 16 ps.

The solution used for the denaturation studies has a very large concentration of ions. From the density of this solution, we calculate that there is about one GndH^+ or Cl^- ion for every three water molecules. To study how such condition affects the bulk-type dynamics in the solution, we measured $C(t)$ in a solution of Trp in 6 M GndHCl solution (Figure 9); for comparison, we also show the result of Trp in buffer solution without GndHCl. A biexponential fit to $C(t)$ for Trp/GndHCl gives $\tau_1 = 570$ fs (28%) and $\tau_2 = 4.4$ ps (72%). The net dynamic spectral shift is 1335 cm^{-1} . These time constants are longer than those of Trp in buffer solution without the denaturant ($\tau_1 = 180$ fs (20%) and $\tau_2 = 1.1$ ps (80%)), but considerably shorter than those of the denatured protein.

The absence of the 16 ps component is evidence of the disruption of the local structure around the Trp site. The observed 56 ps component (which may have other long time components) manifests a much slower “solvation” by the ions and water molecules in collapsed pockets, and by relaxation of the coiled protein structure around the Trp moiety. The large inhomogeneity that exists in these conditions will most likely give multiple solvation times, and the 56 ps component must be taken as an average of these time scales in the time window of our experiments. In fact, our time-resolved Stokes shift shows such inhomogeneity in that parts of the spectra exhibit different probe lifetimes; note that Trp lifetime varies from 340 ps (shortest among the three time constants) in the protein (the other two are ~ 2 and ~ 5 ns) to 500 ps (shortest among two) in the bulk (another one: 3.1 ns).³⁶ The reported times here are much shorter.

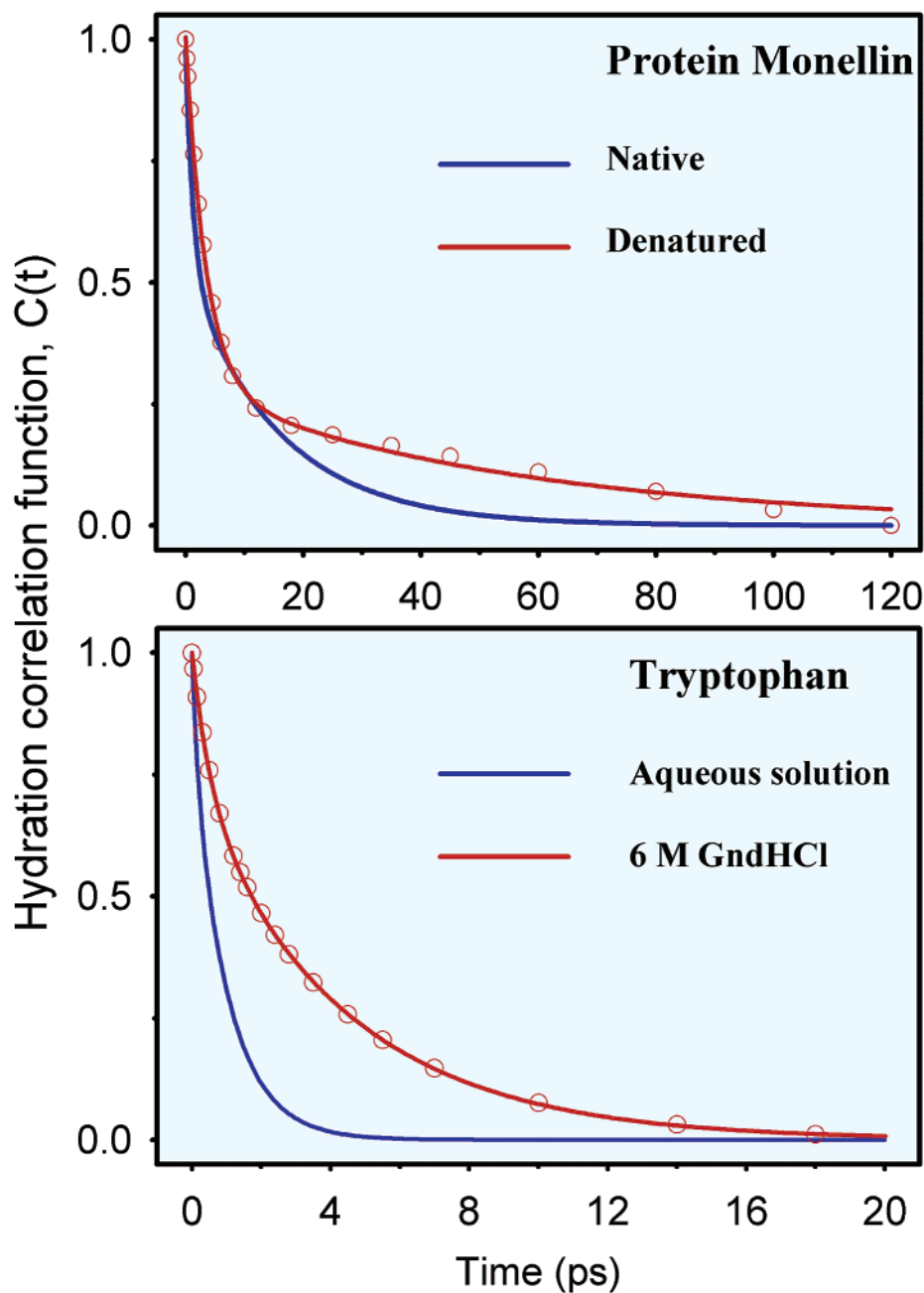


Figure 9. (upper part) Experimental observations giving the hydration correlation function for Monellin in a solution with 6M GndHCl as denaturant. The blue curve corresponds to the solvation function of native Monellin while the red one gives the function of the denatured solution. (lower part) Solvation function of tryptophan amino acid in a 6M GndHCl solution. The blue curve corresponds to the results of bulk water while the red one shows the effect of 6M GndHCl solution on the behavior of free tryptophan. Note the difference in time scales for the upper and lower parts.

Figure 10 shows a space-filling depiction of the native state of Monellin and of two random coil conformations of this protein (only Trp-containing chain B is shown). From the schematic images of the random-coil structures it is expected that the tryptophan moiety has the ability to sample several types of conformations, including those that are exposed to bulk water, hydrophobic cores, and charged sites. In the denatured state, the dynamics of the protein can be described using models developed for polymeric chains.³⁷ For this case, we consider the time correlation function for the chain's solvation energy fluctuations as a multiexponential function:

$$\langle \delta E(0) \delta E(t) \rangle = \sum a_i e^{-t/\tau_i} \quad (18)$$

An approximate estimate of τ_i can now be obtained by assuming a Rouse chain dynamics for a homopolymer.^{37,38} In this model,

the eigenvalues of the normal modes are given by

$$\lambda_l = 3D_0 \left(\frac{l\pi}{Nb} \right)^2, \quad l = 1, 3, 5, \dots, N-1 \quad (19)$$

where N is the number of monomers in the chain, b^2 the mean square bond length, and D_0 is the translational diffusion coefficient of a monomer. For Monellin, $N = 50$. If we assume that an amino acid is a sphere of radius 3 Å, then the estimate of D_0 can be obtained from the Stokes–Einstein relation with a stick boundary condition. We further set $b = 5$ Å. The slowest time can be obtained by setting $l = 1$ in the above expression, giving $\tau \sim 30$ ns. Similarly, the fastest one (with $l = 49$) is on the order of 10 ps.

Such description indicates that there is multiple time scales spanning 3 orders of magnitude for dynamical processes of the

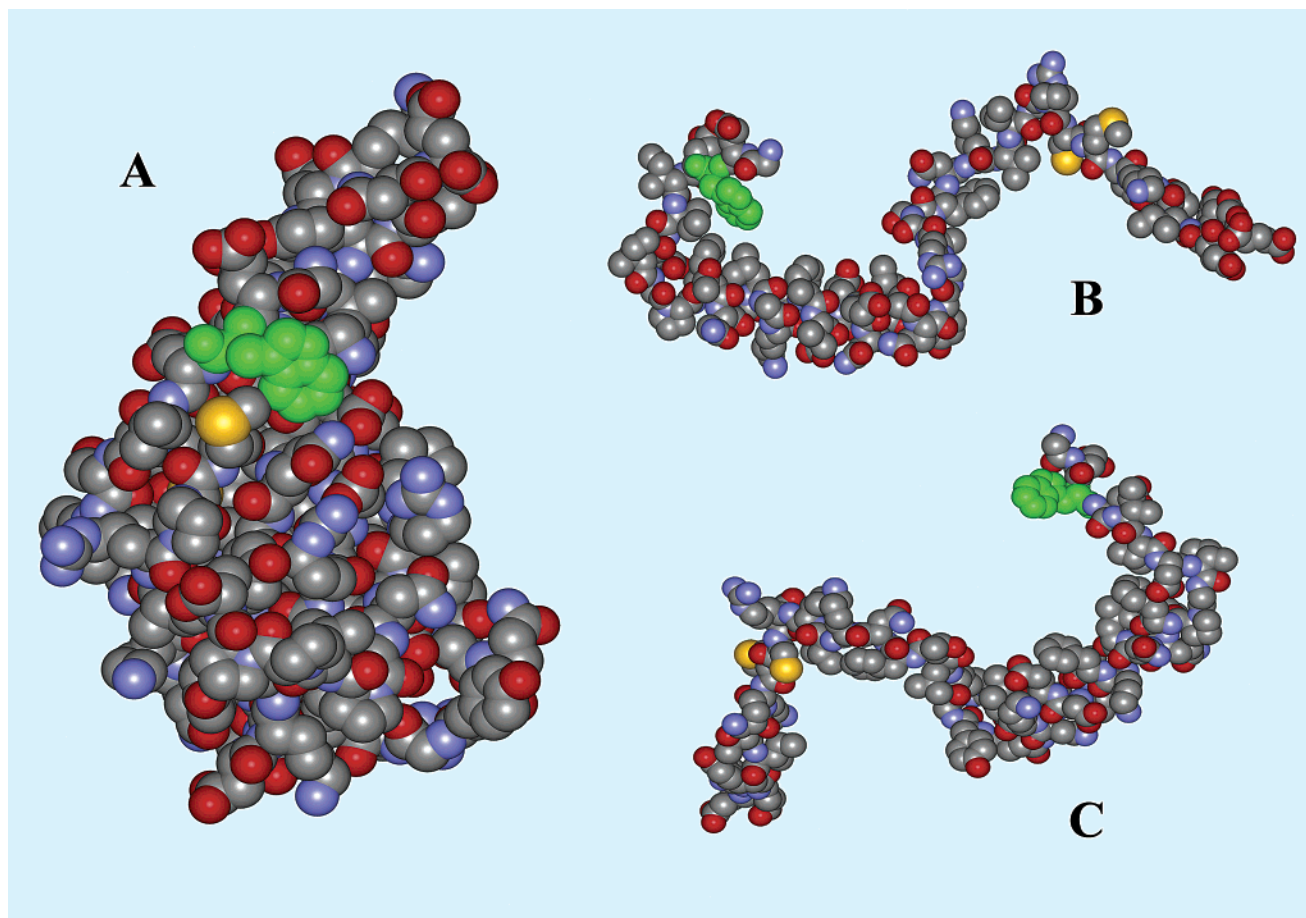


Figure 10. Space-filling models of the protein Monellin in its native state (left) and two denatured random coiled states (right); only the Trp-containing chain B is shown.

polypeptide-random coil. With this in mind, it can be argued that the 56 ps component observed in the $C(t)$ decay of denatured Monellin reflects these fluctuations with an average value in the time window of the solvation experiment. This assumes that the tryptophan chromophore is sensitive, either directly or indirectly through its degree of bulk exposure, to the dynamics of the randomly coiled polypeptide chain. In other words it is the relatively slow motions of the chain (heavily charged) which control the final hydration of the probe.

(D) Biomimetics: Micelles. In water most of the surfactants form almost spherical aggregates when their concentration exceeds certain value, called critical micellar concentration (CMC). These organized assemblies in water, micelles, are often used to mimic the surface effect of proteins.^{10,34} Recently, the analogy with protein dynamics has been given in the review by Bhattacharyya, Bagchi, and co-workers.^{2b,c} As with proteins there exists a slow-component of $C(t)$ which reflects the motions in the bound-water layer.

Experimentally, it is possible to probe the hydration and local rigidity dynamics in the palisade layer of a neutral micelle formed with Triton X-100 (TX-100) from measurements of $C(t)$ and $r(t)$. We used the indole chromophore of *N*-acetyltryptophan amide (NATA), which is a Trp analogue. A small-angle X-ray scattering study³⁹ has shown that TX-100 micelle contains a highly dense palisade layer of water of thickness ~ 25 Å (see Figure 11, upper part for schematic representation). This micellar system can be considered a chemical model to study the hydration phenomenon for the probe-exposed site at a surface in contact with water, similar to proteins.

Figure 11, lower part, shows the experimentally derived hydration correlation function $C(t)$. The time evolution of the

$C(t)$ displays¹⁰ a biexponential decay with time constants of 2.9 ps (45%) and 58 ps (55%). The net dynamic spectral shift is 670 cm^{-1} . The inclusion of NATA in the micelle is confirmed by the dynamical behavior of the anisotropy $r(t)$ (inset of Figure 11, lower part). The persistent $r(t)$ (64%) reflects the absence of rotational tumbling of the probe while the 63 ps decay (36%) probably describes the restricted cone motion of the probe. The observed slow decay in $C(t)$, 58 ps, for the micelle resembles that found in the proteins and the overall response of $C(t)$ is definitely different from that of bulk water. This long decay component of ~ 60 ps is observed over the time scale of our experiment and it is possible that it contains longer time contributions, reflective of a strongly bound water.⁴⁰ The comparison of the micellar surface with that of proteins is not direct, but the important point is that in both cases the dynamical nature of the water layer is evident.

V. Other Aspects of Protein Hydration

(A) Residence Time and Protein Friction. Residence times of water molecules are significant not only for the dynamics and function but also for defining the friction on the protein and its effective volume. We expect the residence time to give a measure of the additional friction on the rotating protein due to the hydration layer. Two limits are clear. When the residence time of the hydration water is very long, even longer than the rotational correlation time of the protein (τ_{RP}), then the friction would increase. The change in friction can be incorporated by increasing the size of the protein since $\xi = 8\pi\eta R^3$, where η is the viscosity of bulk water and R is the effective radius of the protein. The friction ξ is the force correlation function and in

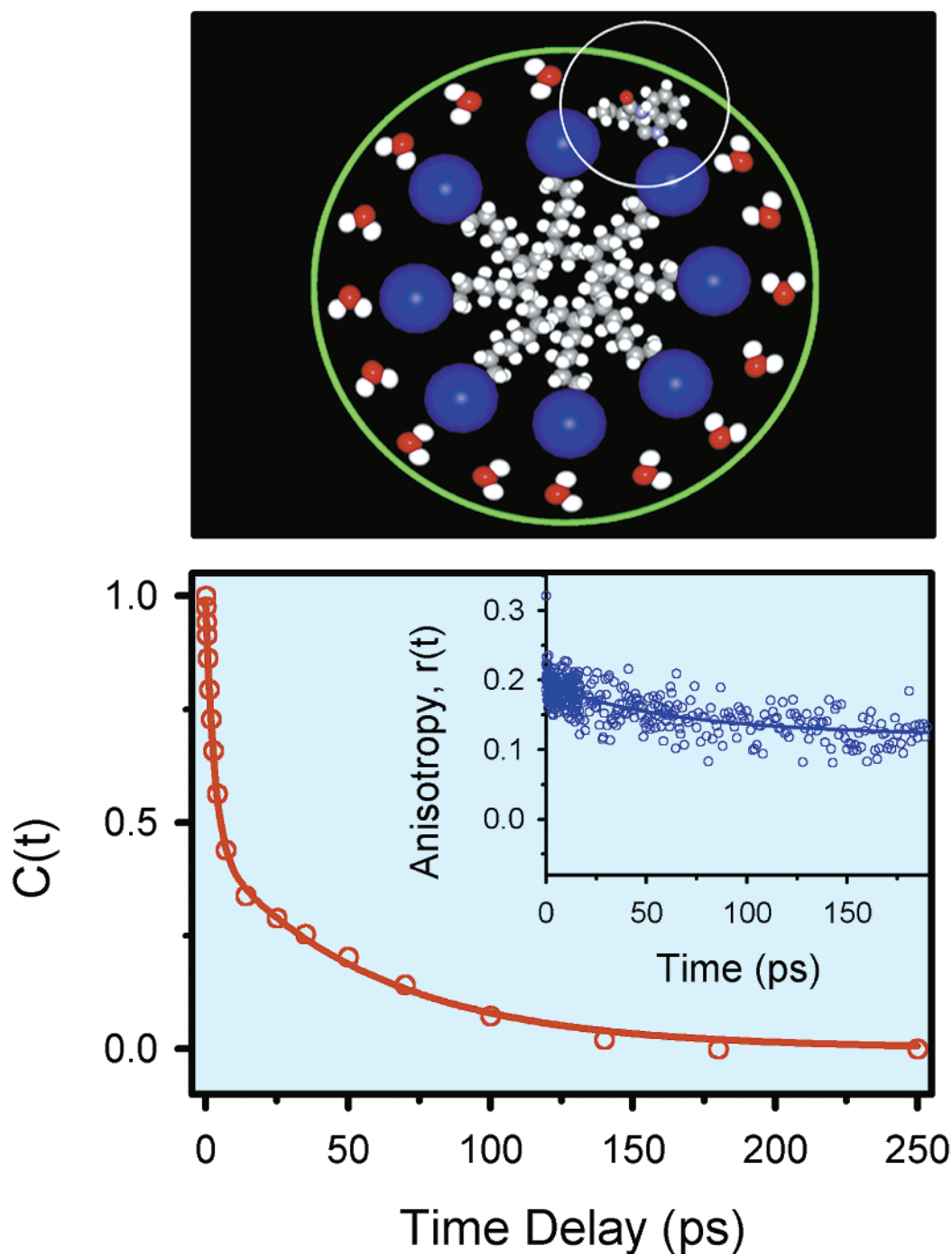


Figure 11. Experimental observations giving the hydration correlation function $C(t)$ (lower part) for *N*-acetyltryptophanamide (NATA) included in a micelle. The time evolution of the anisotropy $r(t)$ shows the restricted motion of the probe molecule, NATA (see text). In the upper part a schematic is shown of the structure.

this case it is determined by the torque for rotation. When the residence time is very short, the effect of the hydration layer will not be felt by the protein. Thus, the ratio of the two times $\tau_{\text{res}}/\tau_{\text{RP}}$ is an important quantity.

In general, one way to proceed is to assume a splitting of the total friction, as is commonly done in dielectric friction theories,⁴¹

$$\xi = \xi_{\text{hyd}} + \xi_{\text{bw}} \quad (20)$$

where ξ_{hyd} is the hydrodynamic contribution which can be equated to the total rotational friction on the protein in the absence of the biological water; it is equal to $8\pi\eta R_0^3$ (hydrodynamic limit) where R_0 is the bare radius of the protein. The

biological water contribution now needs to be calculated microscopically. The biological water friction can be calculated from the torque-torque time correlation function (TTTCF). This TTTCF is proportional to the number of water molecules on the surface which is equal to $4\pi R_0^2 L \rho$ where ρ is the number density in the hydration shell. Using Kirkwood's formula:⁴²

$$\xi_{\text{bw}} = (\beta/3) \int_0^\infty dt \langle T(0)T(t) \rangle \quad (21)$$

where $\langle T(0)T(t) \rangle$ denotes the TTTCF with a standard time averaging and $\beta = (k_B T)^{-1}$. We assume that the decay of the torque occurs by orientation and translation of the water molecules in the layer, which is related to the residence time of

the water molecules. Thus, the biological water friction is given by

$$\xi_{\text{bw}} = \beta(4\pi R_0^2 L \rho) \langle \chi^2 \rangle \tau_T / 3 \quad (22)$$

where $\langle \chi^2 \rangle$ is the mean-square torque by a single water molecule on the protein. Note that the torque correlation time τ_T is closely related to the residence time τ_{res} , which in turn is related to solvation time; note also that the torque correlation function is the same as solvation correlation function when the protein is not moving. ξ_{bw} contains the dielectric friction.

When the size of the protein is very large ($R_0 \gg L$), the hydrodynamic term dominates, as expected and the influence of the hydration layer on the total rotational friction is insignificant. However, when L is significant compared to R_0 , then the contribution from the biological water should be counted, especially if the residence time is long. It is interesting to consider the limit of very long residence time when the hydration layer is that of an ice-like structure. In this case, the mean-square torque from equilibrium fluctuations decreases due to the formation of a well-defined structure on the surface. One can derive a simple relationship for $R_0 \approx L$,

$$\langle \chi^2 \rangle \tau_T = 42\eta/\beta\rho \quad (23)$$

by comparing eq 22 with the total ξ for a radius $R_0 + L$; one recovers the correct limiting friction: that is, R_0 going over to $R_0 + L$ in the hydrodynamic friction. While the above derivation is by no means a complete theory, it clarifies the relation between the friction due to the hydration shell and dynamical quantities such as the residence time. A microscopic calculation of $\langle \chi^2 \rangle$ would require knowledge of surface–water pair correlation function and will necessarily depend on the nature of the binding site. However, the above formulation can be used to obtain an approximate estimate of the relative contribution of the biological water to protein rotational friction.

We consider myoglobin which has a rotational correlation time (from dielectric measurement) of 45 ns (in dilute solutions, ref 9). The use of Stokes friction with the computed radius (16.5 Å) gives a value of rotational correlation time of only 14 ns. The contribution from the hydration layer requires knowledge of the mean-square torque. We assume a simple model where the water molecule with dipole moment μ is located at a distance r from an effective surface charge q_{eff} . The mean-square torque is obtained by averaging over all the possible orientations of the water molecule. The final expression is given by

$$\langle \chi^2 \rangle = \frac{2q_{\text{eff}}^2 \mu^2}{3\epsilon^2(k)r^4} \quad (24)$$

where $\epsilon(k)$ is an effective dielectric constant (not bulk) in the layer and r is an average distance of the water molecule from the charge. When we use $\mu = 1.86$ D, $q_{\text{eff}} = 2$ esu, $r = 4$ Å, $\epsilon(k) = 5$, and $\tau_T = \tau_{\text{res}} = 40$ ps, we obtain from eq 22 the value of ξ_{bw} which is 1.8 ξ_{Stokes} . A total friction of 2.8 ξ_{Stokes} translates to ~ 40 ns for the rotational correlation time, which is close to the observed value. This approximate calculation takes the torque correlation time to be the average residence time.

We end this section by a comment about the applicability of the inhomogeneous continuum models that are often used to explain larger values of solvation time at complex surfaces (micelles, vesicles, oil–water interface, to name a few). The basic idea is that one assigns a dielectric constant to the layer of interface with a reduced value from that of the bulk dielectric

constant ϵ_0 , and/or a longer than bulk Debye relaxation time (τ_D). The expression $\tau_s = (\epsilon_\infty/\epsilon_0)\tau_D$ is then used. Sometimes this procedure is used to provide an estimate of the effective polarity of such surfaces. It should be clear that a surface layer is only a few angstroms thick and the basic assumptions of the standard continuum model are not valid especially if the probe is microscopic in nature.

(B) Residence Time and the Time Scale of Observation.

As mentioned earlier, dielectric measurements give a rotational correlation time of ~ 45 ns for a protein such as myoglobin in solution. Such measurements are sensitive to the motion of the whole protein, and in fact it is the effective volume, including hydration, which is responsible for such long time scales as shown in the preceding section. In the dielectric constant vs frequency response, different regions were found to span the ps to the ns range and for myoglobin two experimental results were reported,⁹ depending on the concentration of the protein: for concentrated solutions, the values are 8.3 ps, 40 ps, 10.3 ns, and 74 ns, assigned to ~ 10 ps (average of 8.3 and 40 ps results) bulk-type relaxation and ~ 10 ns for protein water; for dilute solution only the slow component of 45 ns was reported.

Measurements of the magnetization transfer using nuclear Overhauser effect (NOE) have been involved to obtain a residence time in the hydration layer. The key idea is to relate NOE intensities to the dipole–dipole interaction between protons of the protein and of water (R^{-6}) and to a correlation function describing the stochastic modulation of R that connects the two protons. For the protein bovine pancreatic trypsin, the residence time was reported⁷ to be sub-nanosecond, ~ 300 ps and shorter than 500 ps. This conclusion was supported by a simple calculation. In the initial analysis,⁷ it was assumed that the translational self-diffusion coefficient of water in the layer is only about 1.5×10^{-6} cm²/s. This gave an estimate of the residence time in the same range of 300 ps as that deduced experimentally and this number has been much quoted in the literature. The effective diffusion coefficient, however, ranges from the free water value ($\sim 2.5 \times 10^{-5}$ cm²/s), to *quasi-free*, and to the strongly bound water.

In another series of studies,^{8b} NMR measurements involving water oxygen-17 and deuterium spin relaxation rates have suggested an average residence time in the range 10–50 ps for ribonuclease A, lysozyme, myoglobin, trypsin, and serum albumin proteins. Supported by MD simulations and NOE studies, the time range for the residence in the layer is now given as 10–200 ps.⁸ Following the experimental studies of Halle's group,^{43a} very recent MD simulations by Marchi et al.^{43b} have indicated that the rotational relaxation of water molecules in the close vicinity of the surface of the globular protein lysozyme is retarded significantly (3–7 times) from that of the bulk.

Long relaxation times have recently been obtained²⁹ using three-pulse photon echo peak shift. These experiments provide less than 30 fs time resolution and have been applied to studies of solvation dynamics of eosin dye with the protein lysozyme. The results revealed an 8% slow decay component with time constant of about 500 ps or longer. Although these experiments, like dynamical Stokes shift, probe solvation dynamics, the external dye molecule experiences fluctuations due to the protein and strongly bonded water molecules and both contribute to the decay behavior; the complete X-ray structure of the complex has not been determined but from studies of the protein structure^{44a} and energy transfer with eosin^{44b} it was deduced that the probe is located in a hydrophobic pocket, implying a single site and not an inhomogeneous distribution. As we reach

the ns scale we must consider the relatively slow motions of the protein side chains. Finally, when the probe molecule is larger or comparable to the thickness of the hydration layer, probing of the slow dynamics may become less effective.

VI. Conclusion

In this article we have addressed some key issues of macromolecular hydration with emphasis on proteins in the native and denatured state, and micelles. The femtosecond time resolution provides us with the opportunity of mapping out hydration dynamics on the time scale of the actual molecular motions of water. For two proteins, Subtilisin *Carlsberg* (SC) and Monellin, we used the intrinsic amino acid tryptophan as a single site probe on the surface of the native structure, known from X-ray studies, and we obtained the change in hydration as a function of time through the shift in the spectral properties of tryptophan—at early times, the spectrum is that of a nonequilibrated structure (“blue spectra”) and at longer times it reaches the equilibrium state (“red spectra”). By constructing the hydration correlation function, which represents the solvent energy fluctuation, we obtained the fundamental time constants for solvation. For comparison, we also studied the same probe in bulk water, in the denatured state of the two proteins, and a probe at a distance beyond the layer. The results for the proteins are vastly different from that of the bulk or denatured form and provide the time scales for hydration: ultrafast ~ 1 ps for *free/quasi-free* water molecules and 16 and 38 ps for bound water in the hydration layer of Monellin and SC, respectively.

These fs real time studies of hydration have a spatial resolution determined by R^{-3} between the water and the probe dipole. Using a probe molecule with a dipole gives a better spatial resolution than using a distributed charge because of the R^{-3} dependence, as opposed to R^{-1} for the latter. This brings to focus the following important point, namely, that the definition of a hydration layer is sensitive to the scales of spatial and temporal resolutions intrinsic to the method of probing. Care must be taken to provide the dynamical time scales without convolution from these intrinsic experimental factors.

Theoretical studies of hydration have been made using MD simulations. Here, we provide a simple theory which relates our observations of solvation to the residence times on the protein surface and address the influence of dielectric relaxations, by rotational and translational motions, on the dynamics of bound-to-free water exchange. The latter is critical in view of the fact that the radial distribution function shows a manifestation of structured layer and MD simulations show the equilibration between bound and free molecules. We consider the friction in the layer and its relationship to bulk friction and the consequences to experiments dealing with other time scales.

Hydration of proteins through weak forces is a dynamical process which defines a molecular layer on the scale of a few angstroms. The picosecond time scale of the dynamics excludes a static iceberg type model and it is clear that such ultrafast mobility, by rotational and translational motions, are unique in determining the hydrogen-bonded layer ordering and, hence, the structure and function. For the structure, the hydrophobic collapse in the interior of the protein and the hydrophilic interaction with hydrogen bonded water results in entropic and enthalpic changes which are determinants of the net free energy of stability. The hydrophilic structure in the protein exterior defines the order of the layer.⁴⁵

But the water in the layer has a finite residence time and its dynamics is an integral part of many functions: selective molecular recognition of ligands (substrate) through the unique

directionality and adaptability of the hydrogen bond and water motion; enzymatic activity mediated by water located at the molecular distance scale, not diffusive; and protein–protein association through water mediation by entropic water displacement (desolvation) and energetic minimization of charge repulsion. With this in mind, the time scale for the dynamics is critical—it must be longer than bulk dynamics and shorter than the time for any unfolding of the active structure. To maintain selectivity and order in the layer, the picosecond time scale is ideal. For example, in protein–protein association⁴⁶ the time scale of translational diffusion is $\sim 5 \times 10^{-8}$ s while, as shown above, the residence time is 4 orders of magnitude shorter, allowing for a very effective desolvation and search for the ideal configuration. Accordingly, the present studies promise many new extensions since femtosecond time resolution is ideal for such mapping of hydration, spatially and temporally.

Acknowledgment. This work was supported by the National Science Foundation.

Appendix I

In this appendix, we describe the theoretical model employed and the steps that lead to the derivation of eq 7 of the text. There are several ingredients of the theory. First, of course, is the assumption of the existence of the bound and the free states of water molecules in the layer. This assumption implies the existence of a local equilibrium in the hydration layer and is strictly valid when the binding energy is sufficiently large to make the bound states as an identifiable entity. The fraction of the bound states in the layer is also a function of this binding energy. Second, we assume a simple reaction diffusion equation to describe the interconversion between the bound and the free states and the molecular motion of water molecules. The molecular motions considered are the rotation and translation of water molecules. Third, here we shall ignore the interaction among the water molecules, for two reasons: (a) These interactions are severely perturbed by the protein surface and (b) at the nearest-neighbor distance, density relaxation is well described by diffusion equation. Thus, the effects of interactions on the dynamics are included mostly through the diffusion constants.

With the assumptions, equations of motion are now given by

$$\frac{\partial}{\partial t} \rho_f(\mathbf{r}, \mathbf{\Omega}, t) = D_T \nabla^2 \rho_f(\mathbf{r}, \mathbf{\Omega}, t) + D_R \nabla_{\Omega}^2 \rho_f(\mathbf{r}, \mathbf{\Omega}, t) - k_{fb} \rho_f(\mathbf{r}, \mathbf{\Omega}, t) + k_{bf} \rho_b(\mathbf{r}, \mathbf{\Omega}, t) \quad (\text{A1.1a})$$

$$\frac{\partial}{\partial t} \rho_b(\mathbf{r}, \mathbf{\Omega}, t) = -k_{bf} \rho_b(\mathbf{r}, \mathbf{\Omega}, t) + k_{fb} \rho_f(\mathbf{r}, \mathbf{\Omega}, t) \quad (\text{A1.1b})$$

where ρ_f and ρ_b are the densities of the free and the bound water molecules and the interconversion rates (k_{fb} and k_{bf}) have been introduced earlier. This is a simple Markovian description which can be easily generalized to include memory effects. But memory effects are not expected to play a significant role on the relatively long time scale. In writing the second of the above equations, we have neglected the rotational and translational motions of the bound water molecules. This is again consistent with the assumption of high binding energy. In addition, the rotation and translation of the protein molecule are not included.

The above equations are now solved by the following steps. (i) The densities $\rho(\mathbf{r}, \mathbf{\Omega}, t)$ are expanded in spherical harmonics,

$$\rho_x(\mathbf{r}, \boldsymbol{\Omega}, t) = \sum a_{lm}^x(\mathbf{r}, t) Y_{lm}(\boldsymbol{\Omega}) \quad (\text{A1.2})$$

where $x = f$ or b , (ii) a Fourier transform is performed on the coupled equations, with the momentum variable q being the conjugate to r , and (iii) the quantity of interest for solvation dynamics is $a_{10}(q, t)$. The resulting coupled equations are given by

$$\frac{\partial}{\partial t} a_{10}^f(q, t) = -(2D_R + D_T q^2) a_{10}(q, t) - k_{fb} a_{10}^f(q, t) + k_{bf} a_{10}^b(q, t) \quad (\text{A1.3a})$$

$$\frac{\partial}{\partial t} a_{10}^b(q, t) = -k_{bf} a_{10}^b(q, t) + k_{fb} a_{10}^f(q, t) \quad (\text{A1.3b})$$

The above coupled equations are now solved to obtain eq 7 of the text.

The above treatment should be generalized in many different directions. First, one should include interactions between water molecules so that the equations are valid at smaller wavenumbers. Second, one can include the inertial and the memory terms. In the absence of the protein surface, we have the following general expression for the polarization relaxation:¹⁹

$$P(k, z) = \frac{P(k, t=0)}{z + \sum (k, z)} \quad (\text{A1.4})$$

with

$$\sum (k, z) = \frac{2k_B T f(k)}{I(z + \Gamma_R(k, z))} + \frac{k_B T k^2 f(k)}{m(z + \Gamma_T(k, z))}$$

where $k_B T$ is the Boltzmann constant times the temperature, m and I are the mass and the moment of inertia of the water molecules, and $\Gamma_R(k, z)$ and $\Gamma_T(k, z)$ are the wavenumber- and frequency-dependent rotation and translational friction (or memory) kernels, respectively. In the wavenumber range of interest here, and in the long time limit (z is relatively small),

$$\frac{k_B T}{\Gamma_R(k, z)} \cong D_R, \quad \frac{k_B T}{m \Gamma_T(k, z)} \cong D_T, \quad f(k) \cong 1$$

and we recover the result quoted in eq 4. In a heterogeneous hydration layer, we need to derive a general equation of the above form. One complication (and challenge) is the derivation of expressions for $\Gamma_R(k, z)$ and $\Gamma_T(k, z)$.

References and Notes

- Zewail, A. H. *Angew. Chem., Int. Ed.* **2000**, *39*, 2587.
- (a) Nandi, N.; Bagchi, B. *J. Phys. Chem. B* **1997**, *101*, 10954. (b) Nandi, N.; Bhattacharyya, K.; Bagchi, B. *Chem. Rev.* **2000**, *100*, 2013. (c) Bhattacharyya, K.; Bagchi, B. *J. Phys. Chem. A* **2000**, *104*, 10603.
- (a) Benderskii, A. V.; Eissenthal, K. B. *J. Phys. Chem. B* **2001**, *105*, 6698. (b) Eissenthal, K. B. *Acc. Chem. Res.* **1993**, *26*, 636.
- Michael, D.; Benjamin, I. *J. Chem. Phys.* **2001**, *114*, 2817.
- (a) Kauzmann, W. *Adv. Prot. Chem.* **1959**, *14*, 1. (b) Southall, N. T.; Dill, K. A.; Haymet, A. D. J. *J. Phys. Chem B* **2002**, *106*, 521.
- Finney, J. L. *Faraday Discuss.* **1996**, *103*, 1. See references therein, and the entire issue.
- Otting, G.; Liepinsh, E.; Wüthrich, K. *Science* **1991**, *254*, 974.
- (a) Wüthrich, K.; Billeter, M.; Güntert, P.; Luglinbühl, P.; Riek, R.; Wider, G. *Faraday Discuss.* **1996**, *103*, 245. (b) Denisov, V. P.; Halle, B. *Faraday Discuss.* **1996**, *103*, 227. (c) Halle, B.; Andersson, T.; Forsén S.; Lindman, B. *J. Am. Chem. Soc.* **1981**, *103*, 500.
- Gregory, R. B., Ed. *Protein solvent Interactions*; Dekker: New York, 1995; Chapter 4.
- Pal, S. K.; Peon, J.; Zewail, A. H. *Proc. Natl. Acad. Sci. U.S.A.* **2002**, *99*, 1763.
- Burling, F. T.; Weis, W. I.; Flaherty, K. M.; Brunger, A. T. *Science* **1996**, *271*, 72.
- Cheng, X.; Schoenborn, B. P. *J. Mol. Biol.* **1991**, *220*, 381.
- Gu, W.; Schoenborn, B. P. *Proteins Struct. Funct. Genet.* **1995**, *22*, 20.
- Rocchi, C.; Bizzarri, A. R.; Cannistraro, S. *Phys. Rev. E* **1998**, *57*, 3315.
- (a) Bagchi, B. *Annu. Rev. Phys. Chem.* **1989**, *40*, 115. (b) Fleming, G. R.; Cho, M. *Annu. Rev. Phys. Chem.* **1996**, *47*, 109. (c) Bagchi, B.; Biswas, R. *Adv. Chem. Phys.* **1999**, *109*, 207.
- Jimenez, R.; Fleming, G. R.; Kumar, P. V.; Maroncelli, M. *Nature (London)* **1994**, *369*, 471.
- Onsager, L. *Can. J. Chem.* **1977**, *55*, 1819.
- (a) Wolynes, P. G. *J. Chem. Phys.* **1987**, *86*, 5133. (b) Chandra, A.; Bagchi, B. *Chem. Phys. Lett.* **1988**, *151*, 47. (c) Chandra, A.; Bagchi, B. *J. Phys. Chem.* **1989**, *93*, 6996.
- (a) Roy, S.; Bagchi, B. *J. Chem. Phys.* **1993**, *99*, 9938. (b) Nienhuys, H. K.; Santen, R. A. V.; Bakker, H. J. *J. Chem. Phys.* **2000**, *112*, 8487. The experimental rotational relaxation time is 2.6 ps which gives $D_R = 1.9 \times 10^{11} \text{ s}^{-1}$, close enough to the calculated value in 19a.
- Price, W. S.; Ide, H.; Arata, Y. *J. Phys. Chem. A* **1999**, *103*, 448.
- (a) Stratt, R. M.; Maroncelli, M. *J. Phys. Chem.* **1996**, *100*, 12981. (b) Hsu, C.-P.; Song, X.; Marcus, R. A. *J. Phys. Chem. B* **1997**, *101*, 2546.
- Hynes, J. T. *J. Phys. Chem.* **1986**, *90*, 3701.
- (a) Nagarajan, V.; Brearley, A. M.; Kang, T. J.; Barbara, P. F. *J. Chem. Phys.* **1987**, *86*, 3183. (b) Raineri, F. O.; Resat, H.; Perng, B. C.; Hirata, F.; Friedman, H. L. *J. Chem. Phys.* **1994**, *100*, 1477. (c) Lang, M. J.; Jordanides, X. J.; Song, X.; Fleming, G. R. *J. Chem. Phys.* **1999**, *110*, 5884. (d) De Boeij, W. P.; Pshenichnikov, M. S.; Wiersma, D. A. *Annu. Rev. Phys. Chem.* **1998**, *49*, 99.
- Shen, X.; Knutson, J. R. *J. Phys. Chem. B* **2001**, *105*, 6260.
- Zhong, D.; Pal, S. K.; Zhang, D.; Chan, S. I.; Zewail, A. H. *Proc. Natl. Acad. Sci. U.S.A.* **2002**, *99*, 13.
- Callis, P. R. *Methods Enzymol.* **1997**, *278*, 113.
- Ruggiero, A. J.; Todd, D. C.; Fleming, G. R. *J. Am. Chem. Soc.* **1990**, *112*, 1003.
- Changenet-Barret, P.; Choma, C. T.; Gooding, E. F.; DeGrado, W. F.; Hochstrasser, R. M. *J. Phys. Chem. B* **2000**, *104*, 9322.
- Jordanides, X. J.; Lang, M. J.; Song, X.; Fleming, G. R. *J. Phys. Chem. B* **1999**, *103*, 7995.
- Tarek, M.; Tobias, D. J. *Biophys. J.* **2000**, *79*, 3244.
- Balasubramanian, S.; Bagchi, B. *J. Phys. Chem. B* **2001**, *105*, 12529.
- Zwanzig, R. *Nonequilibrium Statistical Mechanics*; Oxford: New York, 2001; Chapter 4.
- Peon, J.; Pal, S. K.; Zewail, A. H. *Proc. Natl. Acad. Sci. U.S.A.* **2002**, *99*, 10964.
- Zhong, D.; Pal, S. K.; Zewail, A. H. *ChemPhysChem.* **2001**, *2*, 219.
- Tcherkassakaya, O.; Ptitsyn, O. B.; Knutson, J. R. *Biochemistry* **2000**, *39*, 1879.
- Swaminathan, R.; Krishnamoorthy, G.; Periasamy, N. *Biophys. J.* **1994**, *67*, 2013.
- Doi, M.; Edwards, S. F. *The Theory of Polymer Dynamics*; Oxford: England, 1986.
- Srinivas, G.; Sebastian, K. L.; Bagchi, B. *J. Chem. Phys.* **2002**, *116*, 7276.
- Paradies, H. H. *J. Phys. Chem.* **1980**, *84*, 599.
- Pal, S. K.; Sukul, D.; Mandal, D.; Sen, S.; Bhattacharyya, K. *Chem. Phys. Lett.* **2000**, *327*, 91.
- Nee, T.-W.; Zwanzig, R. *J. Chem. Phys.* **1970**, *52*, 6353.
- Boon, J. P.; Yip, S. *Molecular Hydrodynamics*; McGraw-Hill: New York, 1980.
- (a) Denisov, V. P.; Jonsson, B.-H.; Halle, B. *Nature Struct. Biol.* **1999**, *6*, 253. (b) Marchi, M.; Sterpone, F.; Ceccarelli, M. *J. Am. Chem. Soc.* **2002**, *124*, 6787.
- (a) Ramanadham, M.; Sieker, L. C.; Jensen, L. H. *Acta Crystallogr. B* **1990**, *46*, 63. (b) Baugher, J. F.; Grossweiner, L. I.; Lewis, C. J. *J. Chem. Soc., Faraday Trans. 2* **1974**, *70*, 1389.
- Chandler, D. *Nature (London)* **2002**, *417*, 491.
- Camacho, C. J.; Kimura, S. R.; DeLisi, C.; Vajda, S. *Biophys. J.* **2000**, *78*, 1094.
- Morris, J. A.; Martenson, R.; Deibler, G.; Cagan, R. H. *J. Biol. Chem.* **1973**, *248*, 534.